RSC Advances

REVIEW

View Article Online
View Journal | View Issue

Cite this: *RSC Adv.*, 2025, **15**, 13397

Transition metal phosphide/ molybdenum disulfide heterostructures towards advanced electrochemical energy storage: recent progress and challenges

Ali Shahmohammadi,[a] Samad Dalvand,*[b] Amirhossein Molaei,[c] Seyed Morteza Mousavi-Khoshdel,[d] Najmeh Yazdanfar[b] and Mohammad Hasanzadeh *[e]

Transition metal phosphide @ molybdenum disulfide (TMP@MoS_2) heterostructures, consisting of TMP as the core main catalytic body and MoS_2 as the outer shell, can solve the three major problems in the field of renewable energy storage and catalysis, such as lack of resources, cost factors, and low cycling stability. The heterostructures synergistically combine the excellent conductivity and electrochemical performance of transition metal phosphides with the structural robustness and catalytic activity of molybdenum disulfide, which holds great promise for clean energy. This review addresses the advantages of TMP@MoS_2 materials and their synthesis methods—*e.g.*, hydrothermal routes and chemical vapor deposition regarding scalability and cost. Their electrochemical energy storage and catalytic functions *e.g.*, hydrogen and oxygen evolution reactions (HER and OER) are also extensively explored. Their potential within battery and supercapacitor technologies is also assessed against leading performance metrics. Challenges toward industry-scale scalability, longevity, and environmental sustainability are also addressed, as are optimization and large-scale deployment strategies.

Received 18th February 2025
Accepted 8th April 2025

DOI: 10.1039/d5ra01184a

rsc.li/rsc-advances

1. Introduction

Renewable resources have become the new target, considering the need to substitute existing fossil fuel sources as the overall energy demand is increasing.[1,2] This consequently generates a high demand for high-performance energy conversion and storage devices.[3] While solar and wind power are very attractive renewables, their intermittent nature necessitates effective and scalable solutions for storing energy.[4] Batteries, supercapacitors, and hybrid storage devices are the necessary solutions for the challenge but are typically restricted by their high cost, short life cycle, and more considerably their scalability.[5–8]

Heterostructure materials, formed of at least two constituents combined for their synergistic functionalities, have drawn substantial interest.[9–11] TMP@MoS_2 heterostructures are particularly important because they combine the high electrical conductivity and catalytic nature of transition metal phosphides (TMPs) with the structural strength and large molybdenum disulfide (MoS_2) surface area.[12–14] Together, they create synergy, leading to enhanced charge transfer, electrochemical stability, and catalytic activity, thus rendering these composites promising for both electrocatalysis and energy storage devices.[15–17]

TMP@MoS_2 synthesis and characterization improvements have demonstrated their potential for next-generation energy technologies. Various fabrication techniques, such as hydrothermal synthesis,[18,19] electrodeposition,[20–22] and chemical vapor deposition,[23,24] enable the precise engineering of heterostructures with tailored properties.[25,26] The structural and electrochemical properties of the materials are extensively investigated using the techniques of X-ray diffraction (XRD),[27–29] scanning electron microscopy (SEM),[29–31] transmission electron microscopy (TEM),[32] and X-ray photoelectron spectroscopy (XPS)[33,34] to confirm their composition, morphology, and chemical states. Moreover, TMP@MoS_2 heterostructures possess increased efficiencies in such important electrochemical reactions as hydrogen evolution reaction (HER) and oxygen evolution reaction (OER),[2,3,13] that play a critical role in water splitting and fuel cell applications. Though bulk-scale synthesis, interface stability of the materials, and

[a]*Faculty of Chemistry, Kharazmi University, 43 South Mofatteh Avenue, Tehran, Iran*
[b]*Iranian Research & Development Center for Chemical Industries (IRDCI), Academic Center for Education, Culture and Research (ACECR), Karaj, Iran. E-mail: samad.dalvand1398@gmail.com*
[c]*Faculty of Petroleum and Natural Gas Engineering, Sahand University of Technology, Tabriz, Iran*
[d]*Department of Chemistry, Iran University of Science and Technology, Tehran 16846-13114, Iran*
[e]*Pharmaceutical Analysis Research Center, Tabriz University of Medical Sciences, Tabriz, Iran. E-mail: hasanzadehm@tbzmed.ac.ir*

electrochemical durability are needed to commercialize the materials,[35,36] these also need to be accounted for. Herein, we review the recent efforts we made on the TMP@MoS_2 heterostructure from two aspects: the synthesis strategy of TMP@MoS_2 and the electrochemical properties & application. We also discuss the major methodologies used for characterization, highlight the bottlenecks that currently exist in the field, and suggest a set of recommendations for the optimization of the materials for practical applications. By interlinking the fundamental studies with technical applications, the review is focused on delivering useful insights into the role of TMP@MoS_2 heterostructures toward green energy storage and catalysis.

2 Synthesis methods of transition metal phosphides (TMPs), molybdenum disulfide, and TMP@MoS_2 heterostructures

Design and modification of advanced materials like TMP@MoS_2 are mainly done through proper control and modulation of their physicochemical and electrochemical properties to render a well-developed energy storage performance. A suitable choice of synthesis methodology would mark a significant difference in structural stability, conductivity, surface area, and accessibility to active sites. Therefore, materials' scalability, cost, and quality are considered essential concerns for developing and extending the utilization of heterostructures. This section describes in detail various synthesis techniques, their fundamental principles, advantages, and limitations to guide future research and development.

2.1 Ball milling

Ball milling is a mechanochemical method that introduces mechanical force to the materials through grinding balls in rotating or vibrating chambers; breakdown and reformation into nanoscale material occur accordingly. The significant contribution generally comes from high-energy ball collisions with material introducing localized heat and pressure, driving the desired transformations. Therefore, the advantages are: the setup is simple and economy-friendly; it effectively leads to the generation of fine and uniform nanoparticles. Scalability for batch or continuous production is advantageous, whereas potential contamination from milling media is a disadvantage. There is a limitation in tight control of particles' size and morphology, and milling conditions need optimization to avoid degradation.[37–39]

Enabling specific mechanochemical approaches in one-shot or continuous production. The most common batch methods are the shakers pot methods and the planetary mills, and constant processes are often accomplished with twin-screw extruders. The widespread use of TSE in continuous production is partly responsible for the heightened attention toward the use of these mills.[40,41]

Several reviews and research studies documented the available commercial instruments' distinct features and corresponding advantages and drawbacks. For example, shaker mills are simple and efficient only on a small scale; planetary mills give high-energy impacts that reduce fine and uniform particle size.[42,43] On the other side of the spectrum, TSE-based extruders provide continuous production and, thus, are more scalable but are likely to be more complex to set up and run.[44,45]

The equipment and additives selected heavily influence the mechanisms underlying these reactions. Some recent developments introduced new methodologies involving additives for improving reaction simulation or for better outcomes or specified reactivities and have advanced the field significantly. Many studies employ such additives to promote efficiency, reaction pathway control, and desired product features, realizing new improvements in fields such as pharmaceuticals through materials science.[46,47] The constant development of ball milling techniques and careful strategies in using additives underline the dynamics of mechanochemical processes, thus affording many more possibilities for innovations and applications in science and industry.[48–50] Some key parameters that affect ball milling outcomes are Milling Time,[51,52] Ball-to-Powder Ratio (BPR), Rotation Speed, and Milling Atmosphere. The longer timer is equal to a smaller particle size and higher surface area. Excessive milling may also lead to agglomeration, amorphization, or degradation of sensitive materials.[51,53] Increased BPR increases the impact of energy. Thus, particle refinement occurs at higher rates. On the other hand, a high ratio might lead to contamination due to the wearing of milling media.[54,55] Higher collision speeds increase the frequency and energies of the collisions and yield smaller particles,[54,56,57] which enable higher frictional heat and the possibility of damaging phase transition by pressure and heat. Oxidation, reduction, and phase formation are strongly dependent upon inert gas (*e.g.*, Ar, N_2) or chemically reactive environments (*e.g.*, H_2, O_2).[8,11,55] In the process of ball milling, the continuous collision between particles and balls causes local heat and pressure and results in (1) distortion of the lattice and the formation of defects, which enhance the reactivity of the material. (2) Phase transformations, *e.g.*, amorphization or formation of metastable phases.[58–60]

Solid-state reactions by the combination of reactants at the atomic level make chemical synthesis independent of the use of solvents.[28,61] Ball milling is flexible for batch or continuous production.[62,63]

Batch processing (Shaker and Planetary Mills) advantages: high-energy collisions allow for rapid particle size reduction.[10,64] Limitations: Limited throughput with scaling-up difficulties.[65]

Continuous processing (Twin-Screw Extruders-TSE) advantages: it offers continuous production and is suitable for industrial use.[66,67] Limitations: it involves complex setup and process optimization to regulate the reaction (Fig. 1).[71,72]

2.2 Electrochemical deposition (electrodeposition)

Electrochemical deposition is, in principle, based on reducing metal ions from an electrolyte solution onto an electrically conductive substrate under applied potential. Indeed, this technique has been extensively used in preparing thin films and

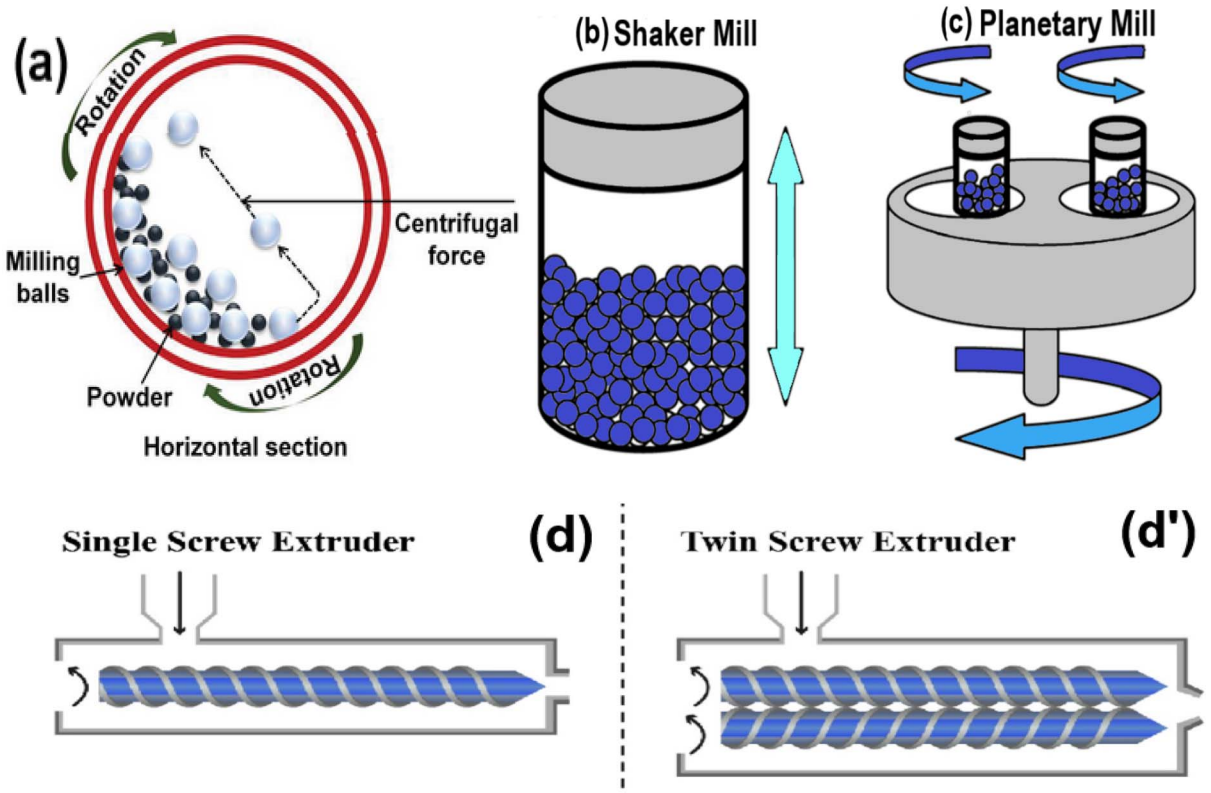

Fig. 1 Schematic representation of (a) ball milling process, (b) Shaker Mill, (c) Planetary Mill, (d) and (d') Single and Twin-Screw Extruder. Reproduced from ref. 68–70 with permission from [Wiely], copyright [2024].

composite materials since it enables excellent thickness and composition control. Advantages: highly controllable process with accuracy in thickness and morphology, inexpensive and easy to handle for laboratory-scale applications, up-scalable for industrial applications, with minimal waste production. Limitations include being only suitable for conductive substrates, uniform deposition over complex, complicated shapes, and deposition rate and material properties dependent upon electrolyte composition and applied conditions.[73–75]

Electrochemical deposition is the electrodeposition process, typically requiring two or three electrodes for better control.[76] During synthesis, conditions like temperature, solution pH, concentration of reactants, and impurity are modified.[77] These parameters influence how fast the material dissolves in an electrolyte, thus affecting deposition.[78] These may alter the dissolution rate of the materials in the electrolyte and thereby affect deposition. It is a comparatively low-cost method by which the thickness of the deposit can be managed, and the desired properties of the coating are obtained.[79] Electrodeposition can deposit large amounts of various materials, including metal-matrix composites, onto substrates.[80] The technique produces materials that enhance the surface properties of corrosion resistance and electrical conductivity for small-scale labs and large industries.[81] However, uniform deposition over complex shapes requires constant concentrations of electrolytes.[82] Optimizing the process parameters avoids cracking or peeling of deposited layers.[83] As they are possibly harmful substances to humans and the environment, electrode position materials must be handled and disposed of safely.[84]

For the TMP@MoS_2 heterostructures, direct deposition with control over film thickness is facilitated by electrodeposition and is a good alternative for hydrothermal and solvothermal methods.[85] Uniform distribution of TMP into MoS_2 is difficult due to varying nucleation rates across the surface.[86] Homogenous coverage and prevention against agglomeration are guaranteed through optimization of the electrolyte concentration, applied potential, and deposition time.[87] Electrodeposited TMP@MoS_2 composites are found as potential supercapacitors and battery candidates with superior electrochemical performances through synergism between the two (Fig. 2).[89,90]

2.3 Hydrothermal/solvothermal synthesis

This technique precipitates the materials from the solution inside the high-temperature and high-pressure autoclave. It is employed extensively for the synthesis of TMP@MoS_2 heterostructures since it is capable of regulating the crystal growth and composition. Hydrothermal and solvothermal synthesis has provided highly uniform and crystalline nanostructures through the regulation of factors like temperature, pressure, and reaction time. In contrast to electrodeposition, the processes here possess better phase purity and uniform structure but require longer synthesis time and higher energy requirements. They have the advantages of being efficient and versatile in the generation of tailored morphologies, being

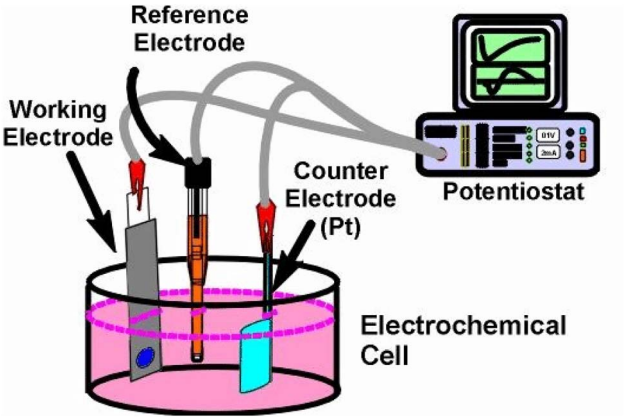

Fig. 2 Schematic of electrodeposition process in three-electrode system. Reproduced from ref. 88 with permission from [IOP Science], copyright [2008].

suitable for large-scale fabrication, and allowing size, phase, and crystallinity to be controlled precisely. Also, limitations include the requirement for high-cost equipment with unique features, such as an autoclave. Reaction times can be long, and lower throughput and Surfactants that are not well controlled might cause the introduction of impurities.[91,92]

One of the most powerful approaches for the synthesis of isolated inorganic compounds in the liquid phase is hydrothermal and solvothermal synthesis.[93] Both approaches facilitate the uniform deposition of TMP onto MoS_2 layers with enhanced electrochemical performance for the function of energy storage. They consist of the reaction between phosphoric materials and metal nitrates or metal chlorides to yield uniform emulsions. The structure is controlled through the incorporation of surfactants into the mixture. The obtained emulsion is subsequently dissolved and recrystallized under high temperatures and pressures within a hydrothermal reactor, *e.g.*, a stainless-steel autoclave lined with Teflon.[94]

During the synthesis process, the vapor saturation pressure is higher than 100 °C, with the autogenous pressure becoming 100 MPa. The high-pressure autoclave produces well-crystallised structures, and therefore, highly pure inorganic compounds are synthesized with high yields. The reaction must be adjusted properly for TMP@MoS_2 to avoid phase segregation and maximize electrical conductivity. Various inorganic compounds like phosphates and complex oxides are prepared using various techniques.[95] Surfactants allow for precise control of the particle morphology and size, improving the material's properties.[96] The methods are also expected to be scaled up for industry and are suitable for research and commercial use.[92] They are ideal for both research and commercial use. The hydrothermal and solvothermal methods, however, have a few disadvantages. The need for extended reaction times (several hours to days) limits rapid material production, which is a drawback compared to faster methods like electrodeposition. As the high temperatures and pressures demanded require unique apparatuses,[97] mainly of an expensive nature and complicated to operate,[98] it is time-consuming since the period taken for dissolution and recrystallization runs into hours.[98] Moreover, other additives and surfactants can be introduced to induce impurities if not regulated.[95] It is also challenging to have homogeneity in TMP@MoS_2 heterostructures due to nucleation rate and reaction kinetic discrepancies at different temperatures and pressures. Lastly, such techniques cannot be applied to inorganic materials of some natures that have a propensity to become unstable under required conditions (Fig. 3).[100]

2.4 Chemical vapor deposition

CVD is a standard method for depositing material or thin films onto substrates by chemical reaction between precursors in the vapor phase. It is widely applied in synthesizing TMP@MoS_2 heterostructures due to the possibility of depositing uniform, high-quality coatings with defined stoichiometry and morphology. This technique has many advantages in terms of

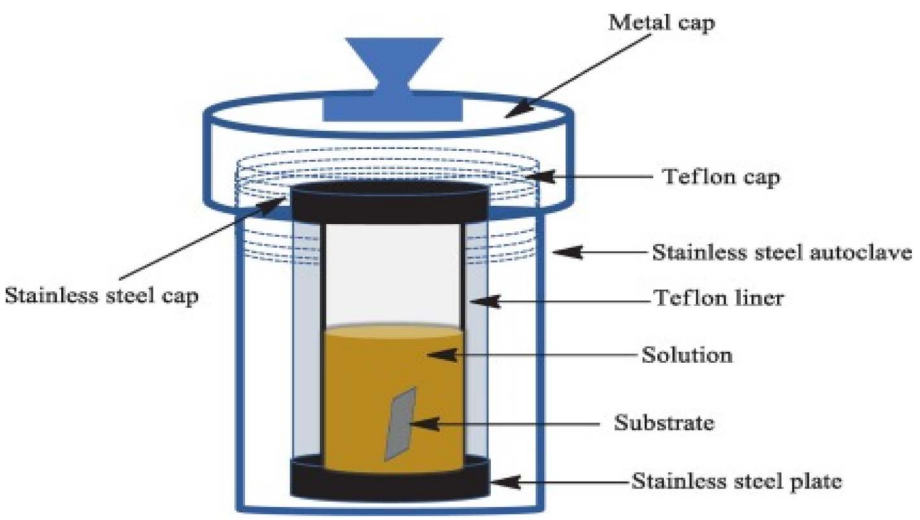

Fig. 3 Schematic of solvothermal technique's equipment. Reproduced from ref. 99 with permission from [Elsevier], copyright [2023].

thickness and stoichiometry control, pure material production, large-format uniform coating, and use with complex geometries. Limitations include high processing temperatures, often complex equipment, and well-controlled reaction conditions in many cases. Moreover, specific precursors can be toxic, highly expensive, and even environmentally hazardous, thus creating problems in handling and waste management.[101–103]

It is an excellent technique for forming ultra-pure, smooth, thin films on heated surfaces through chemical reactions.[101] For TMP@MoS_2, it enables the growth of MoS_2 nanosheets with controlled thickness, facilitating improved electrochemical performance in energy storage applications. Compared with PVD techniques, CVD produces highly uniform and conformal coatings, giving it more flexibility because of the strong bonds to the substrate.[104–106] Nevertheless, CVD has its shortcomings. It is generally accompanied by the application of elevated temperatures, which, if poorly optimized, can lead to phase segregation in TMP@MoS_2 and is restricted by substrate material type.[107] Besides, the choice of TMP precursors is also important in determining nucleation, growth rate, and material properties in general, necessitating optimal selection. Substances used in the process will probably be toxic; therefore, handling and disposal must be done carefully.[108] Additionally, integrating TMP with MoS_2 requires precise reaction conditions to prevent unwanted secondary phases. The complexity increases the equipment costs compared with PVD methods.[109] Despite these limitations, the high regard for CVD has been retained due to its capacity to form exceptionally high-quality films with excellent uniformity, making it virtually indispensable in many industries (Fig. 4).[107]

2.5 Phosphorization methods

The general trend of phosphorization usually includes the conversion of precursors to corresponding phosphides by their reactions in the solid state,[111] gas phase,[112] or solution with active phosphorus-containing agents.[113] Advantages include simplicity, versatility for various phosphides, material properties-conductivity, electrochemical activity, and multiple starting materials.[114] Limitations: the methods in the gas phase require handling hazardous phosphorous gases.[91] Solid-state reactions involve treatment at high temperatures for extended periods.[115] Although very popular, some solution-based techniques always risk producing inhomogeneities with chemical waste.[116]

Phosphorization is one of the most used methods in materials science, mainly for synthesizing metal phosphides applied in electrocatalysis[117] and battery[118] electrodes. Phosphorization within TMP@MoS_2 heterostructures is accountable for the conversion of transition metals to phosphide phases, hence enhancing electrochemical performance by providing improved conductivity and charge transfer kinetics.

There are three major techniques currently in use: solid-state reactions,[119] gas-phase phosphorization,[120] and solution-based techniques.[113] Though simple to carry out and suitable for large-scale production, solid-state reactions require high temperatures and long processing times.[121,122] Requires strict temperature control to prevent unwanted side reactions. Gas-phase phosphorization achieves better control; however, the hazardous gases involved create significant environmental and safety concerns.[123–125] Necessitates advanced containment measures due to toxic precursors. Solution-based techniques have potential because the temperature ranges used are lower[126] and nanostructured materials are possible; however, they often yield inhomogeneous products[127] and chemical waste as by-products.[102,118] Enabling nanostructured TMP@MoS_2 synthesis with tailored morphologies; however, achieving uniformity remains challenging (Fig. 5).

2.6 Ultrasonic method and calcination

Ultrasonic processing and calcination serve critical roles in material synthesis, particularly in enhancing the structural and

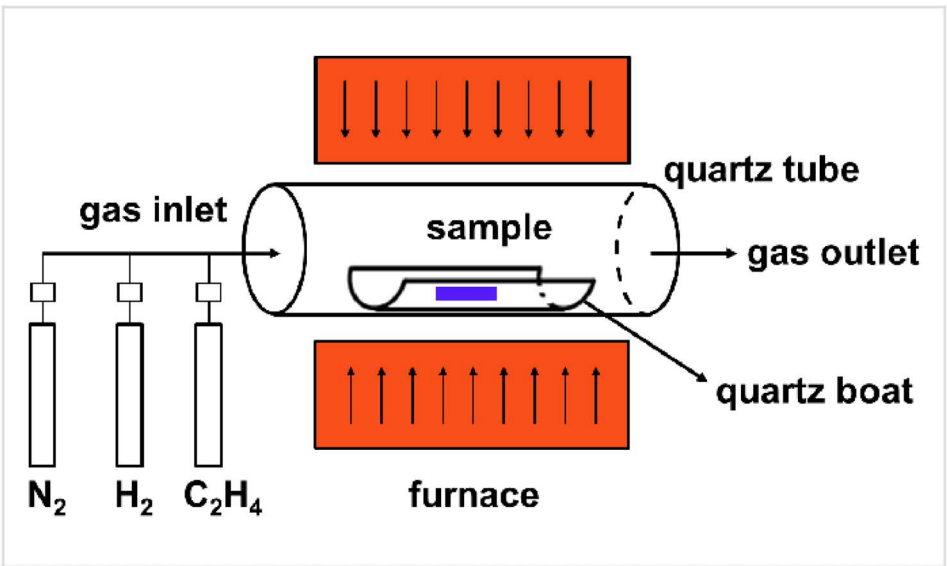

Fig. 4 Scheme of the chemical vapor deposition apparatus. Reproduced from ref. 110 with permission from [Beilstein], copyright [2017].

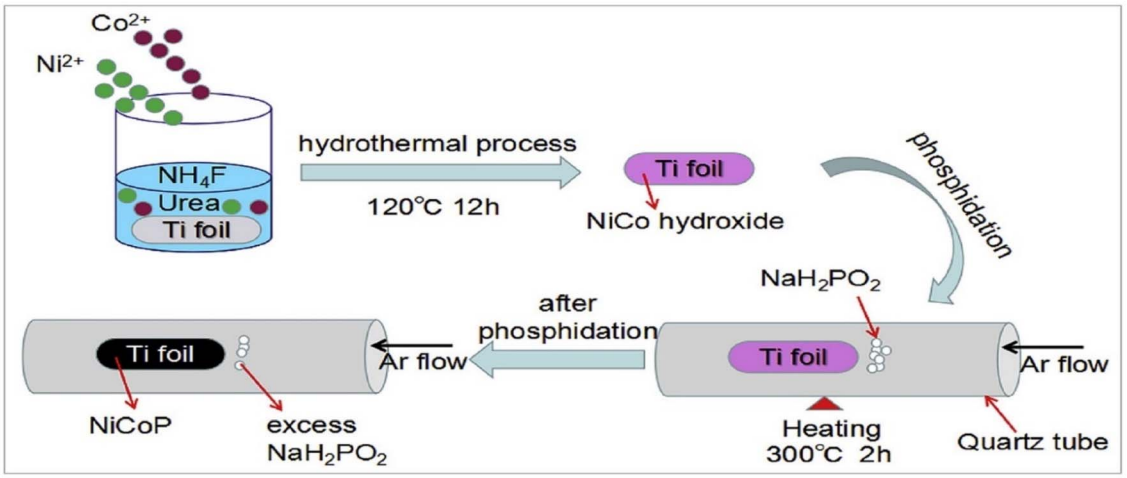

Fig. 5 Phosphorization process for synthesizing NiCoP by NaH_2PO_2. Reproduced from ref. 128 with permission from [Elsevier], copyright [2019].

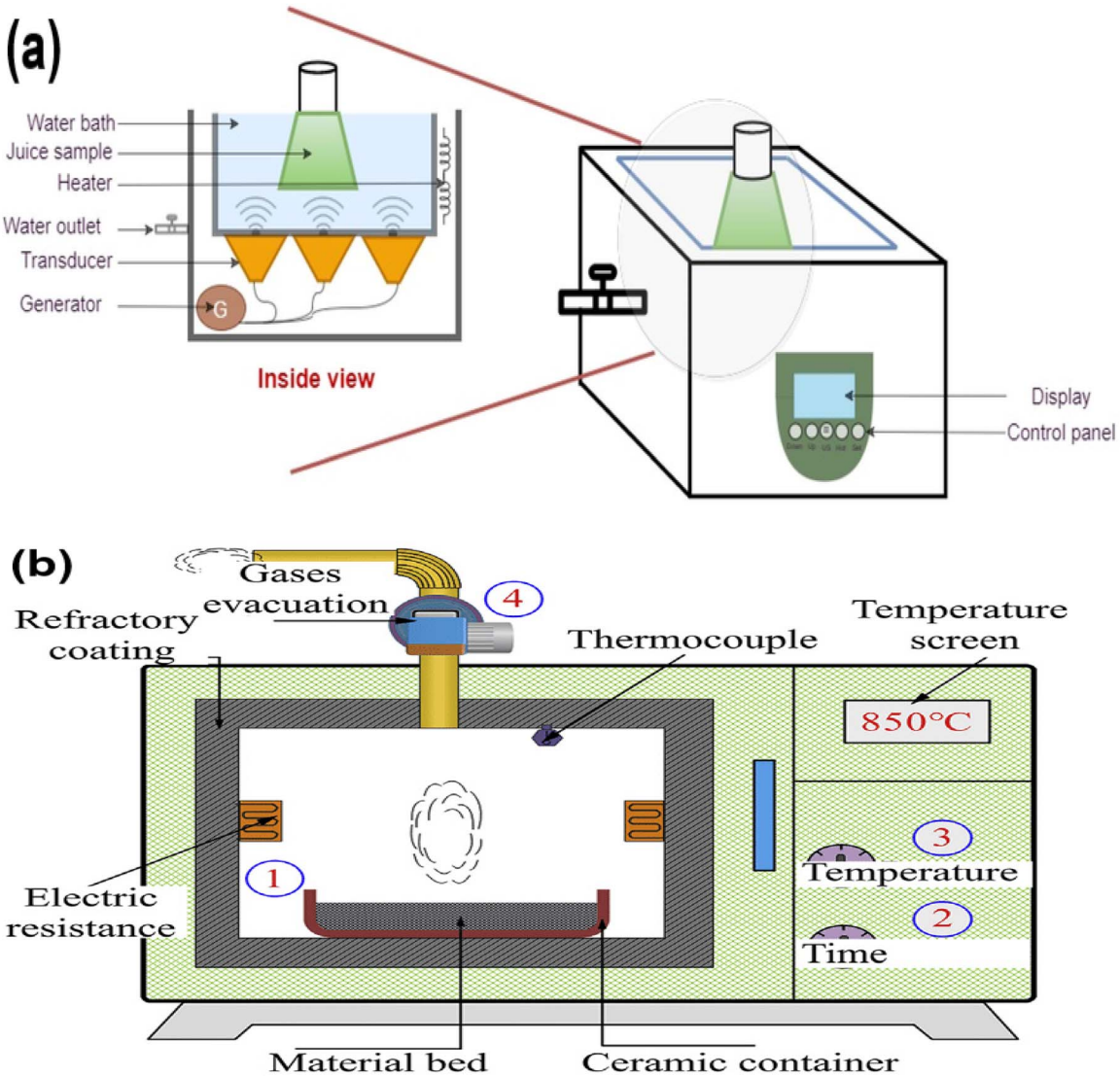

Fig. 6 Schematic of (a) ultrasound system (water bath type), (b) calcination process. Reproduced from ref. 139 and 140 with permission from [Wiely], copyright [2022].

electrochemical properties of TMP@MoS_2 heterostructures. The application of ultrasonic processing has been extensive in the production of fluidic cavitation for chemical reaction intensification.[129] Calcination is generally the heat treatment process for crystallization enhancement and/or removal of impurities from materials.[130] Merits of the ultrasonication method it has fast processing with low energy input. It offers highly homogeneous nanoparticles.[131] Drawbacks: it is non-scalable for large-scale synthesis. It is expensive in terms of equipment for a particular frequency and setup.[132] Ultrasonic processing creates a high-frequency sound that is used in producing cavitation in liquid media, resulting in the collapse of tiny bubbles at a very fast rate. This collapse creates localized pressure and heat. Benefits of calcination: the process enhances material crystallinity and purity,[133] eliminating residues of the impurities and solvent residues.[134] In TMP@MoS_2 synthesis, it facilitates phase transformation and stabilizes the heterostructure. Limitation: the limit to this is high energy consumption with the probability of grain growth; this may reduce the integrity of the nanostructure.[135]

Table 1 Advantages and limitations of different synthesis methods for metal phosphide electrodes in energy storage and electrocatalysis

Synthesis method	Applications (energy storage)	Advantages	Limitations	Ref.
Electrochemical deposition	Batteries, supercapacitors, and electrocatalysts	Fast, low-cost, precise control over synthesis	Requires careful optimization of parameters, limited to conductive substrates	73 and 149–152
Electroless deposition	Batteries, supercapacitors, and electrocatalysts	Simple, scalable, high-quality deposits	Needs surface pretreatment, limited bath life (frequent solution replacement), and environmental concerns	152–155
Photo deposition (photochemical deposition)	Primarily electrocatalysts	Enhanced material properties (crystallinity, conductivity)	Poor reproducibility (results may vary)	156–158
Sonochemical methods	Electrocatalysts, supercapacitors	Improved mass transport, surface cleaning	Complex setup with specialized equipment, limited adoption	159–161
Hydro/Solvothermal synthesis	Batteries, supercapacitors, and electrocatalysts	Efficient, inexpensive, versatile (particle properties)	High pressure & temperature, time-consuming reactions, limited scalability	115 and 162–165
Vapor-phase hydrothermal method	Batteries, supercapacitors, and electrocatalysts	High purity, good scalability	Low yield of material per batch	166–169
Hot-injection method	Batteries, supercapacitors, and electrocatalysts	Narrow size distribution, controlled morphology	Expensive chemicals, challenging to scale up production	144 and 170–172
Solid-state thermal treatment	Batteries, supercapacitors, and electrocatalysts	Potentially simple, scalable, energy-efficient, controlled particle size, wide material range	High temperatures, long reaction times, non-uniform products, limited control over composition, particle agglomeration (increases with complexity)	173
Ball-milling	Batteries, supercapacitors, electrocatalysts	Simple, cost-effective, scalable	Contamination from milling media, limited control over final particle size	174–176
Temperature-programmed reduction	Batteries, supercapacitors, and electrocatalysts	Precise control over reduction conditions, versatile	Requires careful temperature control, sometimes slow	177–179
High-temperature shock	Rechargeable batteries, electrocatalysts	Rapid processing, unique material properties	Potential material degradation, expensive equipment	180
Arc melting	Primarily electrocatalysts	Fast startup, minimal contamination	Compositional inhomogeneity for large samples	144, 172 and 181
Microwave-assisted	Electrocatalysts, supercapacitors	Faster synthesis, lower power consumption	Expensive equipment and limited scalability for large-scale production	172, 182 and 183
Chemical vapor deposition (CVD)	Batteries, supercapacitors, and electrocatalysts	High purity	High temperatures	172, 179, 184 and 185
Plasma-enhanced CVD	Batteries, supercapacitors, and electrocatalysts	Lower temperatures than CVD, better film properties	High equipment cost, complex process	186–188

The process is also referred to as sonochemistry, and it is a process in which material chemistry is altered by exposing it to the application of ultrasonic sound waves with a high frequency.[136] Destabilization of the liquid material is presumed, with very small bubbles forming and collapsing afterward.[137] The collapse is extremely rapid, generating huge pressure and heat, which deposits highly homogeneous nanoparticles with very little energy input.[138] Ultrasonic processing and calcination offer special advantages and restrictions. Ultrasonic processing creates highly uniform ultra-fine nanoparticles with high efficiency. However, restricted sound wave penetration does not support large-scale production. In contrast, calcination creates highly pure, crystalline material. However, it consumes high energy and can degrade product quality due to grain growth and prolonged processing times (Fig. 6).[141,142]

2.7 Other methods

Other common methods for preparing metal phosphides include electroless deposition, which enables uniform coatings without external electrical power;[143] photochemical deposition, which uses light energy to drive reactions, allowing precise nanoscale modifications;[102] or hot injection, provides rapid nucleation and controlled particle growth, essential for tuning morphology.[144] In solid–solid and solid/gas–solid processes, temperature-programmed reduction (commonly used in solid-state and gas–solid processes to reduce metal precursors at controlled temperatures) is usually used;[102] however, joule thermal shock Utilizes rapid heating to synthesize nanomaterials with unique phase compositions,[145] arc melting a high-energy technique to produce dense and crystalline materials,[146] and microwave treatment enables fast, energy-efficient synthesis by selectively heating precursors[147,148] can also be performed. These techniques have often been extensively applied in fabricating supercapacitors, batteries, and electrodes. A comparison between the advantages and disadvantages is presented in Tables 1 to 3. Also, scheme one comparatively analyses all of the synthesis methods, crystal structure (XRD), and morphology (SEM) for MoP/MoS_2, CoP/MoS_2, and CoP/Ni_2P/MoS_2 heterostructures. The dense-packed distribution of the nanosheets suggests the high surface area potential, shown in the SEM image in (a). XRD analysis in (a) shows the successfully synthesized MoS_2 and MoP phases with clear evidence of the heterostructure. This architecture's combination of molybdenum disulfide and phosphide is expected to yield unique properties, enhancing catalytic performance. Heterostructures promise much in many electrochemical applications with their enhanced conductivity, stability, and catalytic activity.

Table 2 Comparison of synthesis methods for metal phosphides@MoS_2 heterostructures: applications, advantages, and limitations

Synthesis method	Applications (energy storage)	Advantages	Limitations	Ref.
Hydrothermal synthesis	Electrocatalysts, supercapacitors, batteries	Simple, low-temperature, cost-effective, tailorable structures	Requires autoclaves, limited crystal growth observation	12, 189 and 190
Phosphorization synthesis	Batteries, electrocatalysts	Enhances LiPS anchoring, improves activity and kinetics	Complex process, limited single-catalyst performance, stability concerns	12 and 191
Emulsion polymerization & pyrolysis	Electrocatalysts	Uniform, stable structures, scalable, high surface area nanostructures	High energy consumption, polymerization control challenges, potential environmental impact	192
Plasma-assisted phosphorization	Electrocatalysts	Fast reactions, uniform coatings, improved catalytic properties	Specialized equipment, high costs, potential safety hazards	193
Electrodeposition	Supercapacitors, electrocatalysts	Precise control over composition and thickness; simple, cost-effective, scalable	Requires conductive substrates, potential adhesion issues, non-uniform deposition	13 and 20
Ultrasonic method & calcination	Electrocatalysts	Enhanced mixing, high surface area nanoparticles, relatively low cost	Uneven particle sizes, high energy consumption, limited scalability	194
Chemical vapor deposition (CVD)	Electrocatalysts	High purity, high control over thickness and composition, scalable	Requires high temperature, expensive equipment, potential safety hazards	195
Solvothermal method	Electrocatalysts	High crystallinity, uniform particle size, tailorable structures	Requires high pressure, long reaction times, limited scalability	196 and 197
Melt-diffusion method	Batteries	High-purity products, straightforward process, high control over diffusion	High-temperature requirement, potential phase separation, limited to specific materials	198
High-temperature carbonization	Electrocatalysts	High surface area, high thermal stability, and enhanced conductivity	High energy consumption, potential environmental impact, complex process	192

Table 3 Synthesis methods for MoS_2: applications, benefits, and limitations

Synthesis method	Applications (energy storage)	Advantages	Limitations	Ref
Hydrothermal synthesis	Electrocatalysts, supercapacitors, batteries	High yield, low cost, controllable morphology	Prolonged reaction time, high pressure required	199–201
Phosphorization synthesis	Electrocatalysts, supercapacitors, batteries	Enhanced electrical conductivity, improved activity	Complex process, use of toxic phosphorous	202–204
Emulsion polymerization & pyrolysis	Batteries, supercapacitors	Uniform particle size, high surface area	Multiple steps require surfactants	205,206
Microwave-assisted	Electrocatalysts supercapacitors batteries	Rapid synthesis, energy-efficient, uniform heating	Limited scalability, expensive equipment	207–209
Electrodeposition	Electrocatalysts, supercapacitors, batteries	Simple, cost-effective, reasonable control over thickness	Requires conductive substrates, lower purity	210–212
Ultrasonic method	Electrocatalysts supercapacitors batteries	Simple, scalable, fast reaction	In inhomogeneous particle size, potential damage to materials	213–215
Chemical vapor deposition (CVD)	Electrocatalysts supercapacitors batteries	High purity, reasonable control over thickness, large-area growth	High cost, complex setup, high temperature	216–218
Solvothermal method	Batteries supercapacitors electrocatalyst	High crystallinity, uniform particle size	Prolonged reaction time requires autoclaves	219–221
Calcination	Electrocatalysts supercapacitors batteries	Simple process, high yield, reasonable control over structure	High energy consumption, potential loss of material properties	222–224
High-temperature sulfurization	Electrocatalyst	High crystallinity, reasonable control over phase	High temperature required, sulfur vapor hazards	225

Based on previous reports summarized in Tables 1–3, the synthesis methods enormously influence the properties and performance of metal phosphide electrodes in energy storage and electrocatalysis. Hydrothermal and solvothermal methods are highly flexible and inexpensive and allow for control over particle properties; however, they often require a very long reaction time and are difficult to scale up. Electrochemical and electroless deposition is inexpensive and fast but substrate-limited and environmentally detrimental. Microwave, sonochemical, and plasma-based methods improve reaction rate and product quality and render them energy efficient but at the expense of highly specific equipment and conditions. Hydrothermal synthesis is still the most popular method to prepare TMP@MoS_2 heterostructures due to its ease and versatility. However, the catalytic properties are auspicious for phosphorization or plasma-assisted techniques. Versatile methods have been used for hydrothermal and chemical vapor deposition in MoS_2 for this material. Simultaneously, these approaches are accompanied by their restrictions on reaction conditions, type of equipment, and product properties. The optimal synthesis route is a function of such factors as desired material properties, cost, scalability, and environmental footprint for a specific application.

In conclusion, this section delved into advanced synthesis techniques to establish a basis for comprehending their practical roles in electrochemical processes, particularly in hydrogen evolution reactions (HER). In this case, materials like the TMP@MoS_2 heterostructure have key structural characteristics and catalyzing efficacy that take center stage in the optimization of HER performance. The essential characteristics, such as improved electron transfer, improved active site exposure, and better structure stability, offer the fundamental platform for optimization in catalysis. Moreover, studies in the acidic and alkaline media point to the importance of such studies in acquiring essential information that can be used in the design of energy-conversion devices.

3. Physical properties of TMP@MoS_2 heterostructures

3.1 Morphology & structural features

The morphologies of the TMP@MoS_2 heterostructures are various, including layered morphologies, nanowires, and core–shell morphologies. For the enhanced hydrogen evolution reaction, core–shell structured CoP@MoS_2 has been employed as an electrocatalyst. In the heterostructure, Maximization of the active site exposure is an available way to offer enhanced catalytic performances. Typically, electron microscopes analyze morphologies; the morphology of the CoCo-PBA possessed a smooth surface with an average particle size ~of about 400 nm. The aggressive PH_3 released by NaH_2PO_2 during the phosphorylation on the nanocubes of the CoCo-PBA produces a rough surface. In the current work, the nanocubes' surface of the CoP-350 was completely covered with nanosheets of MoS_2.[226] Besides, copper phosphate nanowires enriched with phosphorus were reported for use in lithium-ion batteries. XRD pattern of CuP_2 nanowire powder in this form has structures identical to those of AgP_2 with the same space group ($P2_1/c$). All

the diffraction peaks easily characterized the crystalline monoclinic form of CuP_2 with the following lattice parameters: $a = 5.802$ Å, $b = 4.807$ Å, $c = 7.525$ Å, and $\beta = 112.68°$; JCPDS 65-1274. Since CuP_2 is a 10-member ring polyphosphide with a shared edge, some XPS analytical results offered evidence that the CuP_2 nanowires remained stable and oxide-free after being stored in air over a period of more than one month.[227] The triple-layer ternary metal phosphide has been among the layered morphologies that have been utilized to synthesize low-cost efficient bifunctional water-splitting electrocatalysts. Triple-layered ternary metal phosphorite is a typical one of the stacked morphologies that have been utilized in the synthesis of efficient and low-cost bifunctional water-splitting electrocatalysts $Ni_{0.51}$ $Co_{0.49}$ P film has been thoroughly explained in detail. Particles are hundreds of nanometers in diameter, and the shapes of the particles are asymmetrical. The mass transfers the particles to form a uniform type of sheet where the charges are permeable. The particles' surface, where the vertically ordered nanosheets are closely stacked and aligned.[228] In molybdenum disulfide/nickel phosphide, we can observe that XRD patterns of the MoS_2/Ni_2P hybrids are presented in curves, but the diffraction patterns of MoS_2/Ni_2P hybrids consist of a very weak diffraction peak of MoS_2, which indicates that the MoS_2 is amorphous. In addition, the diffraction peaks related to MoS_2 and Ni_2P are observed, thus suggesting the successful combination between MoS_2 and Ni_2P. It may be indexed to proof of the fabrication of the MoS_2/Ni_2P hybrid. Compared with pure Ni_2P, the diffraction intensity of Ni_2P crystal for three MoS_2/Ni_2P hybrids becomes weak. However, with the increase of Ni_2P addition, intensities of diffraction peaks attributed to Ni_2P become strong, and those of MoS_2 show a descending trend, which indicates that Ni_2P plays a major role in the crystallinity of the hybrids.[229,230]

3.2 Electrical conductivity & charge transfer TMP@MoS_2

The electrical conductivity and charge transfer behavior of TMP@MoS_2 heterostructures are essential to their electrochemical activity. While the intrinsic bandgap (~1.8 eV) of MoS_2 results in low conductivity, the presence of metallic TMPs (*e.g.*, FeP, CoP, Ni_2P) enhances the charge transport through minimizing interfacial resistance and enhancing electron mobility. Research has shown that the heterostructures of FeP/MoS_2 surpass those of individual FeP and MoS_2, owing largely to the synergistic interaction between the semi metallic nanoparticles of FeP and the 2D ultrathin nanosheets of MoS_2, acting as a conductive substrate and promoting the transfer of charges. Further, the electrochemical impedance spectroscopy (EIS) verifies that the charge transfer resistance (RCT) in the case of FeP/MoS_2 is much lower compared to that in pure MoS_2, indicating enhanced electron transfer. Further, the turnover frequency (TOF), the density of catalytic sites, and the electrochemical surface area (ECSA) are higher in the case of FeP/MoS_2, which results in enhanced hydrogen evolution reaction (HER) activity. In spite of the lower ECSA due to the possible agglomeration of FeP, the better intrinsic conductivity makes up for the disadvantageous aspect. Density functional theory (DFT) calculations also corroborate the findings, with the Gibbs free energy ($|\Delta G|H$) value for the case of FeP/MoS_2 closer to the optimum value, thus increasing the efficiency in catalysis. These findings prove that the judicious dispersion of the TMP on the substrate of MoS_2 optimizes the conductivity as well as the dynamics of the transfer of charges, making TMP@MoS_2 a suitable candidate for applications involving energy conversion.[231]

3.3 Mechanical properties & structural stability

Mechanical stability in transition metal phosphides (TMPs) is dominated by stoichiometry and bonding in the M–P system. TMPs exhibit both covalency and ionic bonding, making them thermally and chemically stable with high hardness. In metal-rich phosphides ($x:y \geq 1$), metallic conductivity, as well as even superconducting properties, develop due to the occurrence of M–M interactions. High-phosphorus-content phosphides ($x:y < 1$), on the other hand, are characterized by low electrical conductivity and lower stability due to the lack of M–M bonding. Nickel phosphides (Ni_xP_y), for example, demonstrate varying Ni–P coordination with varying P content. An increase in the content of phosphorus leads to the weakening of the Ni–Ni interactions, increasing the distance between the bonds and the formation of P–P dimers. While Ni_2P exhibits higher conductivity, $Ni_{12}P_5$ displays greater resistance to corrosion induced by an acidic environment. These phenomena demonstrate the contribution made by stoichiometry and bonding towards the provision of structural stability for catalysis and for purposes related to energy.[232] Mechanical properties in MoS_2 depend on thickness, structural phase, and pressure. In-plane properties describe monolayers, but stability and function in the case of MoS_2 depend on interlayer interactions in the bulk. MoS_2 exists in various phases (2H, 3R, 1T, 1T′, 1T″) with different electronic and catalytic properties. While the stable semiconductor form exists for the case of 2H–MoS_2, the higher charge transfer properties for the case of 1T-MoS_2 make it suitable for use in electrochemical applications. Pressure also affects the electronic and mechanical properties of MoS_2, making it suitable for lubrication and the storage of energy. Since experimental syntheses of good-quality crystals are difficult, simulations have to be performed computationally to predict mechanical behavior of MoS_2. While it is clear that pressure-induced changes in 2H MoS_2's properties exist, their effect on other phases is poorly understood, suggesting that more research is needed.[233]

3.4 Thermal & chemical stability of TMP@MoS_2

In catalysis and energy storage, the stability of the TMP@MoS_2 heterostructures is the determinant of their efficiency and lifespan.[9] Their long-term durability relies on various factors, including surface property, stability performance, and corrosion resistance.[102]

3.4.1 Phosphidation process & high-temperature effects. The phosphidation process, which forms a critical step in the synthesis of transition metal phosphides (TMPs), takes place at elevated temperatures.[234] The high-temperature process

impacts the crystallinity, phase composition, and the material's morphology.[94] If well controlled, the phosphidation process leads to a highly ordered heterostructure with active sites dispersed uniformly without degrading the layered architecture of the MoS_2.[235,236]

3.4.2 Oxidation resistance. MoS_2, with its antioxidative properties, forms a protective shell that prevents oxidation of the TMPs further on.[237,238] Passivation enhances the long-term stability of the TMP@MoS_2 in the area of electrochemistry and catalysis.[239]

3.5 Surface area & active site exposure

3.5.1 BET surface area analysis & MoS_2 growth. The increase in surface area presents more active sites to the environment, consequently increasing catalytic performance.[240] The BET surface area analysis can also be carried out to investigate the role of MoS_2 nanosheets in enhancing the porosity and surface area.[241] Moreover, the 2D building block nature of MoS_2 yields a highly exposed surface that is favorable for charge and ion transport in energy storage applications.[242]

3.5.2 Edge site exposure & catalytic performance. Compared with the inert basal plane, the edge sites on the MoS_2 are more catalytically active.[243] Vertical growth of the MoS_2 in the heterostructures increases the number of edge sites, which considerably enhances the hydrogen evolution reaction (HER) activity.[244] Edge-dominant catalysis has a significant function in the synthesis of high-performance electrocatalysts.[245]

3.6 Hydrophilicity & wettability in electrochemical reactions

The hydrophilicity of the electrode materials influences their interaction with the electrolyte and, thus, the electrochemical reactions.[246] Hydrophilicity increases the diffusion of ions and the transfer of charges, and the efficiency of the overall electrocatalysis becomes higher.[247] Supercapacitors, batteries, and fuel cells benefit from optimized kinetics through the better wettability found in MoS_2-modified electrodes.[248] Since both Sn_4P_3/Co_2P and MoS_2 possess this characteristic, a heterostructure with both compounds would be expected to result in better wettability.[247,249]

4. Characterization techniques

4.1 Physical characterization

4.1.1 X-ray diffraction (XRD). X-ray diffraction (XRD) is a critical technique for the identification of the crystalline phases of the TMPs (*e.g.*, FeP, CoP)[232] and the MoS_2 (1T/2H polytypes) by the indexation of the peaks, with respect to the reference data, for example, JCPDS 37-1492 for the 2H–MoS_2.[250] XRD also plays an important role in the stability analysis under thermal and electrochemical cycling conditions.[251] The example of XRD analysis results is provided in Fig. 8 in this review paper.

4.1.2 Raman spectroscopy. Raman spectra provide a distinct indication of vibrational modes associated with TMP@MoS_2 heterostructures.[192] Raman spectra of the composites, as well as pure MoS_2, offer valuable information about their structural interaction as well as disorder levels. The appearance of characteristic E^1_{2g} (381 cm^{-1}) and A_{1g} (406 cm^{-1}) Raman peaks indicates the presence of MoS_2, and any shift in the peaks indicates the level of interaction with the supporting matrix.[252] Raman's characterizations also prove the existence of CoP. The 367 and 394 cm^{-1} vibration peaks refer to the in-plane and out-of-plane vibrations of the Mo–S bond, respectively. Moreover, the vibration peak around 228 cm^{-1} is attributed to the Ag. Mode of the Co–P bond, indicating the existence of CoP on the material surface.[253] Raman spectroscopy is a powerful analytical technique for the structural interaction and vibrational properties analysis of TMP@MoS_2 heterostructures. The occurrence of characteristic MoS_2 and CoP peaks confirms their presence and interaction within the composite, demonstrating the power of the Raman analysis in the analysis of the bonding and the material composition.

4.2 Morphological and microstructural analysis

4.2.1 Scanning electron microscopy (SEM). The morphologies of the samples prepared are normally examined using SEM, and FESEM, and transmission electron microscopy (TEM). SEM findings of the hierarchical tubular MoP/MoS_2 composite include information about its tubular nature.[254] Additionally, it provides information on particle size, such as Molybdenum disulfide-coated nickel–cobalt sulfide with a nickel phosphide core–shell structure.[255]

4.2.2 Transmission electron microscopy (TEM). Transmission Electron Microscopy (TEM) is commonly used to analyze the structural and morphological properties of TMP@MoS_2 heterostructures. Additionally, Energy Dispersive Spectroscopy (EDS),[256] in combination with TEM, provides elemental composition information.[257]

For instance, in syntheses of molybdenum phosphide (MoP) nanorods with graphene assistance on silicon, high-resolution TEM (HR-TEM) micrographs indicate distinct fringes of a well-defined lattice with *a* spacing of 0.278 nm corresponding to hexagonal Mop's (100) plane. Furthermore, the fast Fourier transform (FFT) pattern also confirms the high crystallinity of MoP nanorods to authenticate their structure.[258]

4.3 Chemical and electronic structure

4.3.1 X-ray photoelectron spectroscopy (XPS). X-ray photoelectron spectroscopy is a powerful method for the study of various phenomena in gases, liquids, and solids. X-ray photoelectron spectroscopy provides information on local physical phenomena in X-ray photoemission, facilitating spectrum modeling and derivation of vital information such as core-level line shapes, binding energies, built-in potentials, and band-edge discontinuities in complex oxide heterostructures. The binding energy and shape of a photoemission peak are influenced not only by the atomic number, valence, and orbital of the ejected electron but also by intricate many–body interactions that occur during the photoemission process.[259]

XPS analysis showed CoP@MoS_2-75. The binding energies of Mo 3d and S 2p in CoP@MoS_2-75 were displaced from those of pure MoS_2. The Mo and S shifts were approximately consistent (~1 eV) due to the presence of Mo–S bonds, which is attributable

to the strong contact between MoS_2 and CoP. The binding energies for the Mo 3d and S 2p in the CoP@MoS_2-75 were shifted away from those for pure MoS_2. The shifts for the Mo and S were about the same value (~1 eV) as a result of the presence of the Mo–S bonds due to the close contact between the MoS_2 and the CoP. The shift in binding energy and the other fitting peaks in the Co–S bands in the spectra for the Mo 3d and the S 2p (Fig. 6(a) and (b)) attest to the strong bonding contact between the CoP and the MoS_2, possibly enhancing the HER activity of the MoS_2.[15]

4.4 Electrochemical characterization

This evaluation typically employs a three-electrode system comprising a saturated calomel reference electrode, a platinum plate counter electrode, and the as-prepared working electrode. These techniques are cyclic voltammetry (CV), galvanostatic charge–discharge (GCD), and electrochemical impedance spectroscopy (EIS). They can be used to evaluate the electrochemical performances of supercapacitors,[260] electrocatalysts,[261] and batteries.[262] These methods are beneficial to detect improvement of electrochemical performances in heterostructure; for example, the CV curves of FeCoP/CC, NiCoP/CC, and FeCoP@NiCoP/CC electrodes at a scan rate of 5 mV s^{-1} display a growth on redox peaks with apparent potential separation. Additionally, the GCD curves exhibit a longer discharge time in the case of FeCoP@NiCoP/CC. EIS can evaluate the reaction kinetics and the electrical conductivity. In this case, the FeCoP@NiCoP/CC electrode exhibits the lowest R_s value of 0.624 Ω, compared to 0.638 Ω for the FeCoP/CC electrode and 0.655 Ω for the NiCoP/CC electrode. These results demonstrate the significant improvement in electrochemical performance achieved through heterostructures.[263] Therefore, all these measurements are crucial for evaluating the performance and efficiency of energy storage equipment.

4.4.1 Cyclic voltammetry (CV). CV is a fundamental technique to examine the redox behavior, capacitance, and charge storage mechanism of TMP@MoS_2 heterostructures.[264] In this technique, cyclic sweeps of the working electrode occur at a preset voltage range, and the current is recorded.[265] The curvature of the CV curves provides valuable information on charge storage kinetics, pseudocapacitive contribution, and reversibility of reactions.[266–268]

For TMP@MoS_2 materials, their CV curves will show a combination of faradaic redox peaks and non-faradaic double-layer charging dependent on the heterostructure composition.[269,270] The scan rate dependency of the CV curves also provides information on charge transfer kinetics with higher scan rates leading to higher capacitive currents.[271]

4.4.2 Galvanostatic charge–discharge (GCD). GCD measurements consist of subjecting working electrodes to current densities that are constant and measuring voltage response with time.[272] The technique provides valuable information on specific capacitance, energy density, power density, and cycling stability.[273] The charge–discharge behavior of TMP@MoS_2 heterostructures can be linear (capacitive) or nonlinear (pseudocapacitive/faradaic).[274] Higher capacitance is seen in a longer discharge time at a given current density.[275] Cycling stability of TMP@MoS_2 electrodes is determined by subjecting electrodes to repeated charge–discharge cycling and monitoring capacity retention with time.[276]

4.4.3 Electrochemical impedance spectroscopy (EIS). Electrochemical Impedance Spectroscopy (EIS) is utilized to examine charge transfer resistance, ionic diffusion kinetics, and interfacial properties of TMP@MoS_2 heterostructures.[277–279] EIS measurements include imposition of AC voltage perturbations over a range of frequencies and measurements of resultant current response.[280] The impedance data is represented in a Nyquist plot with high-frequency semicircle due to charge transfer resistance (R_{CT}), and low-frequency tail due to diffusion phenomena of ions.[281] EIS fitting optimizes electrode structure to increase charge transfer and decrease resistance to increase electrochemical performance in batteries and supercapacitors.[282]

5. General mechanisms of heterostructures in energy storage and catalysis

5.1 General mechanisms in supercapacitors

Energy storage has been the backbone of all renewable energy systems in modern times, acting as a link between generation and consumption.[283] Supercapacitors have emerged as a critical component because they can store energy rapidly and release it with a very long cycle life.[284] This differs from batteries in that supercapacitor energy storage is done through purely electrostatic mechanisms, consequently allowing faster charge and discharge processes.[285] This section describes the supercapacitor performance based on electrical double-layer capacitance, pseudocapacitance, and a hybrid mechanism for their potential role in developing energy storage solutions for high-power and sustainable applications. In general terms, there are three ways through which energy is stored in all electrochemical supercapacitor types, which are introduced below.

5.1.1 Electrical double-layer capacitance (EDLC). The electrical double-layer capacitor (EDLC) is an electrolytic energy storage device that works at the interface between an electrode and an electrolyte. When voltage is applied, ions from the electrolyte collect near the electrode surface and produce two oppositely charged layers. Because the space is so small, the capacitance value becomes very high (Fig. 7). This is why EDLCs are very useful in applications requiring quick storage and energy release, such as quick bursts of power supply.[287]

5.1.2 Pseudocapacitance. Pseudo-capacitance mainly involves energy storage *via* fast reversible redox reactions at or close to the electrode's surface. In contrast, EDLCs store energy through electrostatic charge separation, while pseudocapacitance lies in between where faradaic electron transfer across the electrode–electrolyte interface is supposed to occur (Fig. 8). This type of behavior has been observed in nanomaterials, conducting polymers, and transition metal oxides.[289]

5.1.3 Hybrid supercapacitors. Hybrid supercapacitors have gained the attributes of batteries and symmetric supercapacitors, with the ability to store bulk energy and power capability. This device drives faradaic and non-faradic

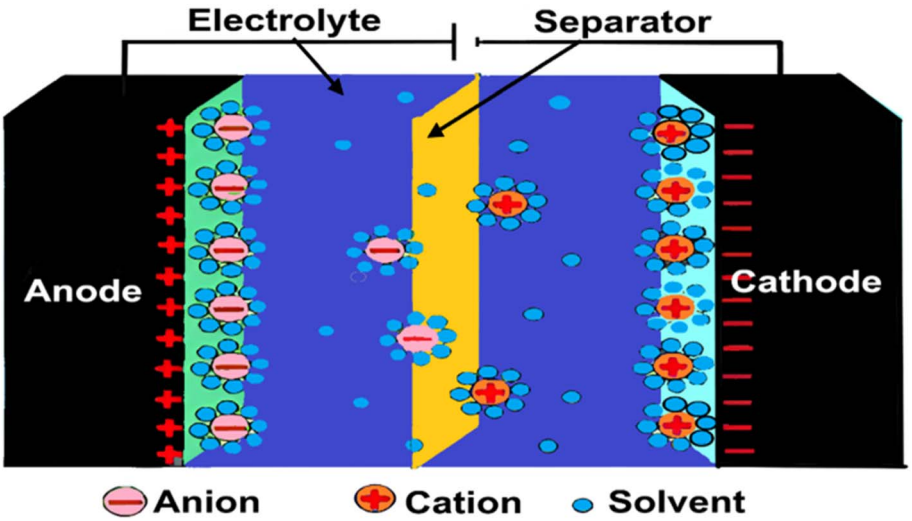

Fig. 7 The structure of electrical double-layer capacitance. Reproduced from ref. 286 with permission from [IOP Science], copyright [2022].

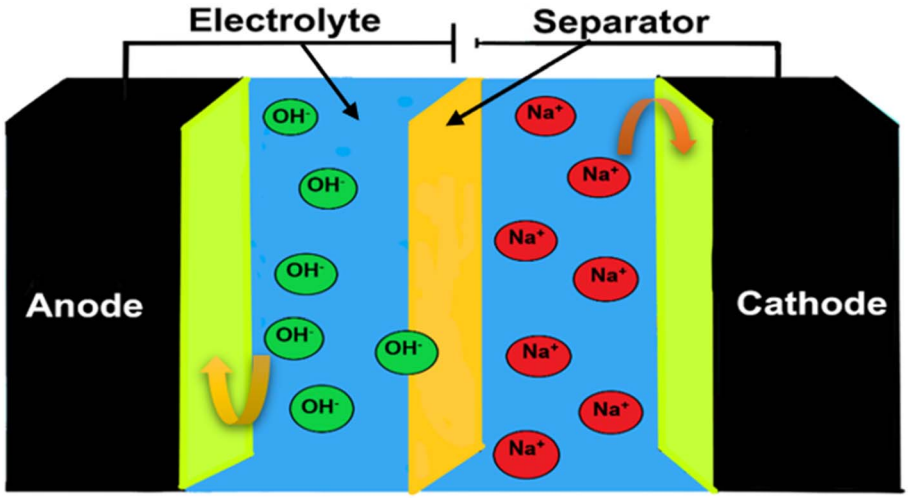

Fig. 8 The mechanism structure of pseudocapacitance. Reproduced from ref. 288 with permission from [Royal Society of Chemistry], copyright [2021].

processes that again eliminate the inadequacy of every technology. In this way, developing new electrode materials in the future, improving electrolytes, and trying asymmetric electrode configurations will become essential strategies (Fig. 9) for further performance enhancement to achieve their applicability in all forms of energy storage devices.[290]

5.2 General mechanisms in batteries

Batteries operate on the principle of the electrochemical mechanisms converting chemical energy to electrical energy. The major electrochemical mechanisms in batteries are classified into different processes: redox reactions (reduction–oxidation reactions), also called faradaic reactions,[291] generate current through a redox reaction on the working electrode surface. The second process is called ion transport through the electrolyte,[292] whereby, upon discharge, ions flow through the electrolyte from one electrode to the other to balance the charge made by the electron flow in the external circuit.[293] The type of ions that flow depends on the chemistry of the battery. For example, in lithium-ion batteries, lithium ions (Li^+) migrate from the anode to the cathode during discharge.[294] The third mechanism is electrode processes. In sure batteries, like lithium-ion batteries, the active ions (*e.g.*, lithium ions) are inserted into or extracted from the electrode materials during charging and discharging.[295] Here, two phenomena are involved: Intercalation, the insertion of ions inside the electrode matrix, usually during the charging process,[296] and deintercalation, the removal of ions from the electrode matrix, usually during the discharging process.[297,298] And the electrical double layer (non-faradaic processes) does not include the transfer of charge and occurs inside the electrode.[299] During the process, the charges of the ions accumulate on the surface of the working electrode, forming and discharging a double-layer

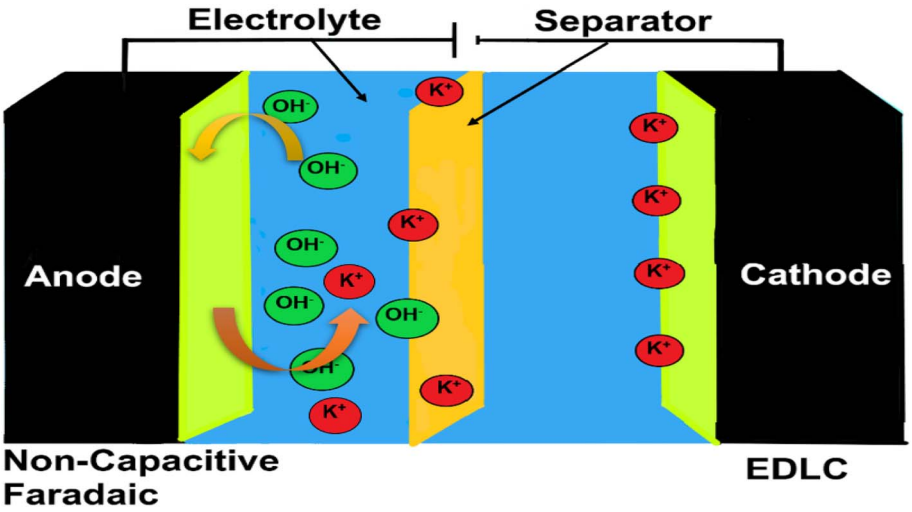

Fig. 9 The structure of hybrid supercapacitors, Reproduced from ref. 288 with permission from [Royal Society of Chemistry], copyright [2021].

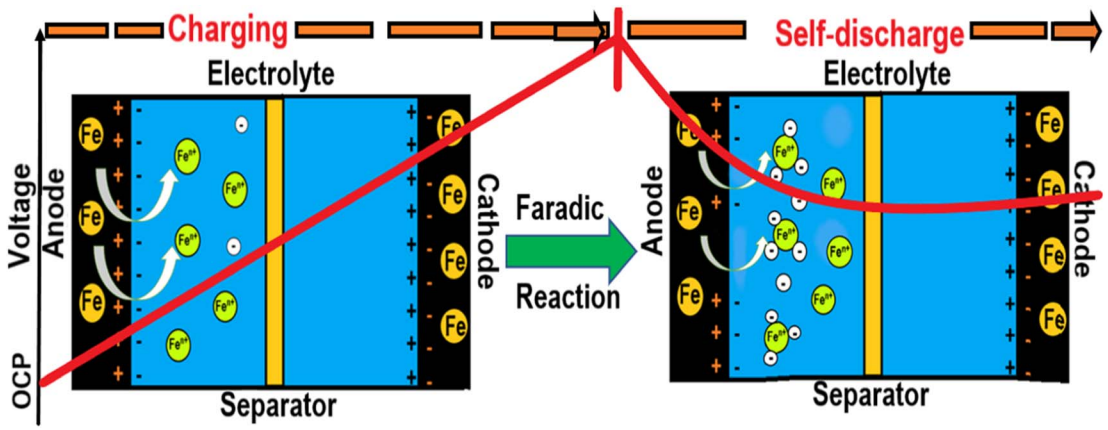

Fig. 10 Faradaic reaction process in batteries, Reproduced from ref. 300 with permission from [JEC], copyright [2021].

capacitance. The attachment of the target biomarker on the electrode surface modifies the dielectric constant of the double-layer capacitance (Fig. 10 and 11).

5.3 General mechanisms in electrocatalysts

5.3.1 General mechanism of HER in acidic and alkaline media. The hydrogen evolution reaction is significant in water electrolysis and is a substantial process for sustainable hydrogen production.[302] Hydrogen, a clean energy carrier, is vital on the road to renewable energy systems for global energy demands.[303,304] In this respect, understanding the HER mechanism is of prime importance in designing efficient catalysts that operate effectively in different media.[305,306] HER has to overcome complex problems, such as the dissociation of water in highly alkaline conditions, when its kinetics are faster in an acid environment.[305] These sections discuss the mechanisms of acid and alkaline mediums with and upon metal surfaces and illustrate the balance of adsorption and desorption processes toward efficiency and applicability thanks to catalysts.

HER serves as the other half of the water electrolysis process. In an acidic environment, hydrogen atoms are absorbed onto the surface of the applied catalyst during the hydrogen evolution reaction (HER), later combining to form molecular hydrogen. The process is relatively efficient and safe.

$$H^+ (aq) + e^- \rightarrow H_{ads} \quad (1)$$

$$\text{Low } H_{ads} \text{ coverage: } H_{ads} + e^- + H^+ (aq) \rightarrow H_2 (g) \quad (2)$$

$$\text{High } H_{ads} \text{ coverage: } H_{ads} + H_{ads} \rightarrow H_2 (g) \quad (3)$$

On the other hand, she happens in a much more complex way in alkaline conditions. In this case, water first has to dissociate its molecules to provide the protons needed in the reaction, so the process is done step by step, therefore taking time compared to acidic conditions. Thus, the most efficient catalysts for HER need to take control of the adsorption and desorption of the intermediate molecules at the catalyst surface under alkaline conditions.

$$\text{Volmer step: } H_2O (aq) + e^- \rightarrow H_{ads} + OH^- \quad (4)$$

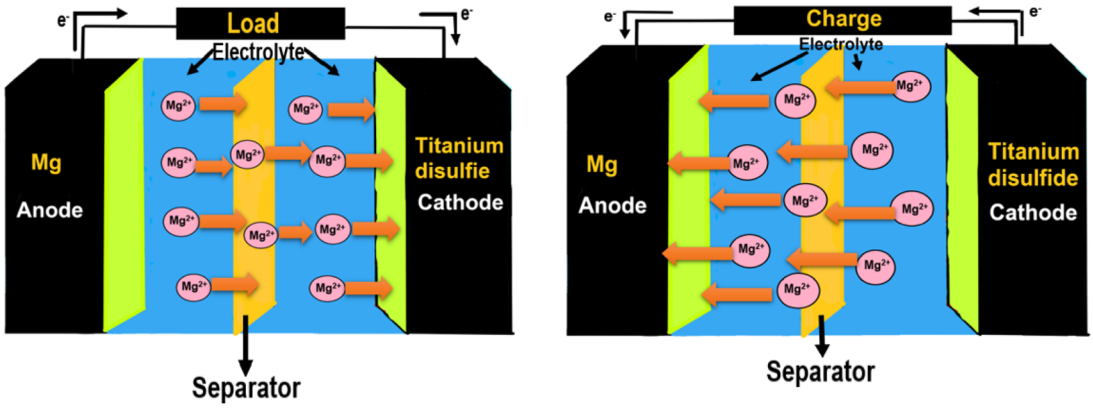

Fig. 11 Ion transport in batteries, Reproduced from ref. 301 with permission from [Nature], copyright [2021].

$$\text{Heyrovsky step: } H_2O\ (aq) + e^- + H_{ads} \rightarrow H_2 + OH^- \quad (5)$$

$$\text{Tafel step: } H_{ads} + H_{ads} \rightarrow H_2\ (g) \quad (6)$$

Although the pathways followed in acidic and alkaline media differ, HER is the central process of water electrolysis. HER is highly efficient in acidic media, and the reverse is the case in alkaline media, where water dissociation proves deleterious to HER. To develop a catalyst that can proficiently handle the adsorption and desorption of molecular species under an alkaline condition, an effective HER is imperative in further developing this technology.[307–309]

Following the comprehensive examination of HER mechanisms in Section 3, the focus will shift to the corresponding half-reaction in water electrolysis—the oxygen evolution reaction (OER). As the counterpart to HER in hydrogen production, OER generates oxygen, playing a crucial role in shaping the overall efficiency of the electrolysis process. A thorough understanding of HER mechanisms also sheds light on the obstacles and potential strategies for optimizing OER, as both reactions rely on energy-efficient rates driven by the ideal balance of adsorption and desorption characteristics.

5.3.2 General mechanism of OER in acidic and alkaline media. While protons in acidic mediums may be favorable for the reaction, hydroxide ions under alkaline conditions grow into different problems.[310,311] The following section describes the mechanism of OER in both acidic and alkaline conditions and how advanced catalysts have significantly improved reaction efficiency and stability toward sustainable energy technologies.

The most likely mechanism for reactions in acidic media is as follows:

$$2H_2O \rightarrow O_2 + 4e^- + 4H^+ \text{ the overall reaction} \quad (7)$$

$$2H_2O + * \rightarrow OH^* + H_2O + H^+ + e^- (\Delta G_1) \quad (8)$$

$$OH^* + H_2O \rightarrow O^* + H_2O + H^+ + e^- (\Delta G_2) \quad (9)$$

$$O^* + H_2O \rightarrow OOH^* + H^+ + e^- (\Delta G_3) \quad (10)$$

$$OOH^* \rightarrow O_2 + H^+ + e^- (\Delta G_4) \quad (11)$$

The oxygen evolution reaction (OER) is a complex process involving four electron transfers. It occurs gradually, sequentially forming intermediate compounds OH*, O*, and OOH*. It is relatively slow. Many articles have investigated the detailed mechanisms of the OER in acidic or alkaline environments.

In alkaline media:

$$4OH^- \rightarrow O_2 + 2H_2O + e^- \text{ the overall reaction} \quad (12)$$

$$4OH^- \rightarrow OH + 3\ OH^- + e^- (\Delta G_5) \quad (13)$$

$$OH^* + 3OH \rightarrow O^* + 2OH^- + H_2O + e^- (\Delta G_6) \quad (14)$$

$$O^* + 2OH^- + H_2O \rightarrow OOH^* + OH^- + H_2O + e^- (\Delta G_7) \quad (15)$$

$$OOH^* + OH^- + H_2O \rightarrow O_2 + H_2O + e^- (\Delta G_8) \quad (16)$$

where * is the active site, OH*, O*, and OOH* are the intermediates adsorbed on the site, and G is the change in Gibbs free energy.[312]

6. Specific mechanisms of TMP@MoS_2 in different applications

The TMP@MoS_2 heterostructures' high efficiency in catalysis and energy storage results due to the synergistic structural and electronic properties in the heterostructures. Transition metal phosphides (TMPs) possess good electrical conductivity, while molybdenum disulfide (MoS_2) exhibits high surface area, chemical stability, and active site richness. The mechanisms underlying their efficiency are due to the increased charge transfer, interfacial synergy, and optimized adsorption and desorption kinetics of the ions.

In batteries, the presence of the TMPs enhances the diffusion of the sodium/lithium ions by expanding the interlayer spacing and lowering the resistance to the transportation of the ions, whereas the storage of the charges through the intercalation and the conversion reactions is facilitated by the presence of the MoS_2. In the case of electrocatalysis, the electronic band structure of the

MoS_2 gets regulated by the presence of the TMPs, aligning the d-band center at the Fermi level to lower the energy barrier for the HER/OER. The interaction between the TMPs and the MoS_2 becomes strong, enhancing the better adsorption of the reactant as well as the more efficient transfer of the electron, enhancing the efficiency of the catalyst tremendously. In the case of the supercapacitors, the pseudocapacitive storage and the fast diffusion of the ions through the TMP@MoS_2 heterostructures enhance the cycling stability and the energy density. The synergy in the integrated system optimizes the storage of the ions, the redistribution of the charges, and the catalysis and is found to be highly suitable for the future generation of electrochemical applications.

6.1 Mechanisms in supercapacitors

Unlike most current literature, which attributes MoS_2's capacitance primarily to electric double-layer capacitance, studies on current response and scan rates reveal that the capacitance of few-layered MoS_2 mainly originates from intercalation pseudocapacitance. Integrating TMPs further enhances electrical conductivity and introduces additional redox-active sites, improving capacitance and energy density.[313] The conductivity is enhanced with the addition of TMP, and more redox sites are added, thereby enhancing the capacitance and the energy density.[314]

Hybrid supercapacitors (HSCs) are drawing attention due to their ability to combine two unlike electrodes with different mechanisms for the storage of charges with high energy density without compromising power output. Transition metal phosphides, and specifically bimetallic nickel cobalt phosphide (NiCoP), are promising as the HSC positive electrode due to their redox sites, high reversibility in the electrochemical process, and stability even over extended periods of time. The electrochemical properties of NiCoP can be further optimized with rationally designed heterostructures, elemental doping, and nanocomposite morphologies to improve the efficiency in the storage of the charge in HSCs.[315]

As mentioned above, molybdenum disulfide (MoS_2) is made by two sheets of S sandwiched between Mo by van der Waals forces. This configuration creates a large surface area and provides the intercalation of ionic species with the electrolyte without causing any crystal structure deformation, resulting in pseudocapacitive charge transfer.[316] So, Combining MoS_2 with TMPs in hybrid supercapacitors leverages the high-power density of capacitors and the high energy density of batteries. The result is products with improved performance parameters for a range of applications in multiple areas of energy storage. This simple principle increases the natural conductivity, active sites, and synergistic interactions among the individual units of the TMP@MoS_2 heterostructure, making the latter more efficient in the storage and conversion process of energy (the excellent performances of the new-generation batteries, electrocatalysts, and supercapacitors combine the best performances of the three factors).

6.2 Mechanisms in batteries

One of the benefits of transition metal phosphides on batteries is ensuring abundant adsorption–diffusion–conversion interfaces for accelerating LiPS transformation and Li_2S deposition, which cause to extremely decreases the accumulation of LiPSs in the electrolyte and, therefore, prevents the migration of LiPSs. The ultrafine Ni_2P nanoparticles prove this is happening.[317] Also, they suggested good electrical conductivity and dual adsorption-conversion capabilities. By increasing electrical conductivity and providing additional active sites for lithium insertion, they are considered a promising cathode host for new-generation LSBs.[318] By using molybdenum disulfides, the less stacked layers can lead to a large specific surface area, enhancing electron transfer and exposure of active sites.[319] Moreover, it was mentioned that TMPs contribute to improved capacity and cycling stability.[320]

In Sodium-Ion Batteries (SIBs) similar to LIBs, transition metal phosphides lead to expanded interlayer spacing, accommodating larger sodium ions and enhancing diffusion kinetics. This structural modification leads to improved electrochemical performance.[321]

6.3 Mechanisms in electrocatalysts

The exceptional catalytic activity of the transition metal phosphides (TMPs) arises due to their optimized electronic structure, rich active sites, as well as efficient electron transfer capability. Phosphorus adjusts the d-band center and the Fermi level, promoting reactant adsorption and desorption of the products. The HER is regulated by the P atoms and is enhanced by oxy/hydroxides or phosphates that are created *in situ* to enhance OER. Defect sites are introduced by P doping that enhances active site concentration. Metal-rich phosphides (*e.g.*, Co_2P) are more conductive and enhance catalytic efficiency. The blending of the TMPs with MoS_2 creates a heterostructure that has high conductivity as well as rich active sites, enhancing catalytic activity and stability towards advanced electrocatalysis.[146]

The blend of the TMP with the MoS_2 forms a heterostructure that takes advantage of the high conductivity of the TMP and the richness in active sites of the MoS_2. The catalytic activity and stability are enhanced through this combination, and it has the potential to be a new way forward for advanced electrocatalysis. The nature of the active sites has been treated in Coordination Chemistry Reviews (Volume 506, 1 May 2024, 215715) in the review article The Nature of Active Sites of Molybdenum Sulfide-Based Catalysts for Hydrogen Evolution Reaction by Weifeng Hu and coauthors.[322]

7. Electrochemical performance of TMP@MoS_2

The electrocatalytic performance of MoS_2/TMP heterostructures is enhanced through interface engineering and charge redistribution, thereby optimizing the hydrogen evolution reaction (HER)[15] and oxygen evolution/reduction reactions (OER/ORR).[323] The metallic 1T-MoS_2 phase in TMP@MoS_2 facilitates hydrogen adsorption ($\Delta G\_H^* \approx 0.06$ eV) *via* sulfur vacancies and strained Mo–S bonds.[324] Notably, MoS_2@CoP/CC exhibits low overpotentials of 64 mV and 282 mV for HER and OER, respectively, in alkaline solution, along with a HER

overpotential of 72 mV@10 mA cm^{-2} in H_2SO_4. Furthermore, P–MoS_2@CoP/CC, as a bifunctional catalyst, delivers relatively low cell voltages of 1.83 V and 1.97 V@500 mA cm^{-2} in 30% KOH, demonstrating high catalytic efficiency for overall water splitting.[325] Tafel kinetics confirm a Volmer–Heyrovsky mechanism,[326] and flower-like Co–Ni–P/MoS_2 heterostructure hybrid spheres show excellent overall water splitting performance in an alkaline solution with a low Tafel slope of 71 and 41 mV dec^{-1} for oxygen and hydrogen evolution reactions.[323]

Specific studies on MoS_2/metal phosphide heterostructures for supercapacitors are limited, but phosphorus doping in MoS_2 has shown promising results. However, our previous research paper introduced nickel cobalt phosphide/Molybdenum disulfide on nickel foam as an effective electrode material in a supercapacitor. The capacitance achieved was 2352.40 F g^{-1} at 1 A g^{-1}, which is exceptionally high. Its high energy density (52 W h kg^{-1} at 321 W kg^{-1}) and power density of 321 W kg^{-1} made it great for applying supercapacitors.[20] Furthermore, researchers recently suggested that phosphorus-doped molybdenum disulfide regulated by sodium chloride be used for advanced supercapacitor electrodes. This study was synthesized using phosphomolybdate acid as a molybdenum source and an *in situ* dopant and sodium chloride (NaCl) as a structural regulator. A maximum capacity of 564.8 F g^{-1} at 1 A g^{-1} and retaining 56.3% of the original capacity at 20 A g^{-1} was achieved.[327] For this reason, this review paper was suggested to give information on the gap research of this heterostructure on supercapacitors and batteries. This can be the novelty of this work and study on the heterostructure of TMP@MoS_2.

A flower-like heterostructured MoP–MoS_2/PCNFs hierarchical nanoreactor was introduced in Li–S batteries, which enhanced kinetics. This study revealed that this composite shortened the lithium-ion channel, shuttle, and fast LiPS conversion ability due to abundant anchoring sites of MoP–MoS_2 heterojunction nanoflowers.[12] This heterojunction exhibits 1090.02 mA h g^{-1} and a high discharge capacity of 884.67 mA h g^{-1} even after 300 cycles at 1C, which compared to molybdenum disulfide alone with a high reversible discharge capacity of up to 994.6 mA h g^{-1} for the MoS_2-1 electrode and 930.1 mA h g^{-1} for the MoS_2-2 electrode is incredibly high.[328]

8. Energy storage applications of TMP@MoS_2

8.1 Lithium/sodium-ion batteries

Bimetallic phosphide Ni_2P/CoP@rGO heterostructure was used in batteries, and this heterostructure delivers an ultrahigh capacity of 196.4 mA h g^{-1} at 10 A g^{-1} after 5000 cycles for lithium-ion batteries and 103.7 mA h g^{-1} at 3 A g^{-1} after 800 cycles for sodium-ion batteries.[329] Yolk–shell tin phosphide composites demonstrated superior electrochemical performance. The capacity of Li-half cells was 521.2 mA h g^{-1}, which was maintained after 3000 cycles at 5.0 A g^{-1}. This amount for Na-half cells is 203.1 mA h g^{-1} maintained after 300 cycles at 1.0 A g^{-1}.[330] Micro–nanostructure designed CoP@MoS_2 delivers a high initial discharge capacity (1321 mA h g^{-1} at 0.1C), high rate capability (837 mA h g^{-1} at 2C), and stable cycling performance (0.101% capacity decay after 250 cycles at 0.5C), suggesting great application prospects of the micro–nanostructure catalyst in Li–S batteries.[16] CoP–C@MoS_2/C heterointerface enhanced Lithium/Sodium Storage exhibits outstanding long-cycle performance of 369 mA h g^{-1} at 10 A g^{-1} after 2000 cycles. In SIBs, the composite also displays an excellent rate capability of 234 mA h g^{-1} at 5 A g^{-1} and an ultra-high-capacity retention rate of 90.16% at 1 A g^{-1} after 1000 cycles.[331] MoS_2/MoP Mott–Schottky heterostructures in lithium–sulfur batteries as promising material deliver an initial capacity of 919.5 mA h g^{-1} with a capacity of 502.3 mA h g^{-1} remaining after 700 cycles at 0.5C. Even under higher sulfur loading of 4.31 mg cm^{-2} and a lower electrolyte to sulfur (E/S) ratio of 8.21 μL mg^{-1}, the MoS_2/MoP@rGO@S cathode could still achieve good capacity and cycle stability.[332] These observations show the huge promise of metal phosphides when incorporated with MoS_2 for improving energy related devices based on lithium-ion, sodium-ion, and lithium–sulfide batteries with much greater electrochemical properties. The improved capacity, cycling stability, and high-rate capability validate the effective implementation of metal phosphides with MoS_2 in tackling the larger issues for conductivity and structural stability, offering possible solutions for the evolution of novel energy-storage devices.

8.2 Supercapacitors

Several surveys have been conducted on the heterostructure of transition metal phosphides with metal sulfides; however, few have been explicitly related to molybdenum disulfide. An example is NiCoP@CoS tree-like core–shell nanoarrays on nickel foam, which serve as high-performance electrodes for supercapacitors. These NiCoP nanowire-based electrodes with electrodeposited shell layers of CoS nanosheets possess a high value of specific capacitance of 1796 F g^{-1} at a current density value of 2 A g^{-1} with a high value of cycling stability as 91.4% retention for 5000 cycles. The asymmetric supercapacitor based on NiCoP@CoS and activated carbon has an energy density value of 35.8 W h kg^{-1} at a power density value of 748.9 W kg^{-1}.[333] Yet another instance: the use of Ni–Co oxide/phosphide/sulfide (NCOPS) composites in nanowire arrays on Ni foam exhibits a specific capacitance value of 2915.6 F g^{-1} with a retention value of 80.39% of the specific capacitance value for 4000 cycles of constant current as 5 A g^{-1}.[334] Further, the hierarchical porous heterostructure Ni_2P/NC@$CoNi_2S_4$ with a high value of specific capacitance as 2499 F g^{-1} at the value of current density as 1 A g^{-1} is another instance, with a capacitance retention value as 91.89% for the value of 10 000 cycles. In this case, it exhibits an impressive value of value of energy density of 73.68 W h kg^{-1} at the value of power density of 700 W kg^{-1}.[335] However, few papers on the heterostructures of the transition metal phosphide/molybdenum disulfide are found. Out of those, we recently reported the electrochemical synthesis of a hybrid nanostructure of nickel cobalt phosphide/molybdenum disulfide on nickel foam, as reported in our previous research work.[20] These findings reflect the impressive

advancement in the transition metal phosphide/sulfide heterostructures towards the application in the field of supercapacitors. However, the scarcity of papers on the phosphide/molybdenum disulfide heterostructures reflects the novelty in the current work, establishing the unique promise of NiCoP/MoS_2 towards high-performance energy storage devices.

8.3 Electrocatalysts

8.3.1 Hydrogen evolution reaction (HER). Fortunately, there is much more research about TMP@MoS_2 and its application to the Hydrogen Evolution Reaction (HER). Hierarchical cobalt–nickel phosphide/molybdenum disulfide is a good example related to HER, and the results showed that this heterostructure led to improved electrochemical performance. The optimized CoP/Ni_2P/MoS_2–CC sample shows low overpotentials of 335, 119, and 211 mV at 100 mA cm^{-2} in neutral, alkaline, and acidic electrolytes with small Tafel slopes of 63, 62, and 82 mV dec^{-1}, respectively.[13] Hollow CoP@MoS_2 hetero-nano frames are another example that showed a low overpotential of 119 mV at 10 mA cm^{-2}, a small Tafel slope of 49 mV dec^{-1}, a large electric double-layer capacitance of 10.28 mF cm^{-2}, and prominent long-term stability.[15] MoP/MoS_2 heterogeneous structure with rich S-vacancy, which revealed excellent catalytic activity and good cyclic stability, showing a lower Tafel slope of 60 mV dec^{-1} at a current density of 10 mA.cm^{-2} and no potential attenuation after the cyclic stability test for 24 h.[336] S-scheme boron phosphide/MoS_2 heterostructure in water splitting photocatalysts application.[337] These results demonstrate the vast potential of TMP@MoS_2 heterostructures towards the Hydrogen Evolution Reaction (HER), with their high catalytic activity, low overpotentials, and exceptional stability. The range of reported structures demonstrates the versatility of TMP@MoS_2 in electrochemical applications, confirming its significance in sustainable hydrogen production.

8.3.2 Oxygen evolution reaction (OER). The research about this heterostructure in Oxygen Evolution Reaction (OER) is not as much as Hydrogen Evolution Reaction (HER). MoS_2‖CoP heterostructure loaded on N, P-doped carbon. The excellent electrocatalytic activity was expressed and also mentioned. This work proposes a novel and facile strategy to prepare the heterostructure compound and serves as a good reference for constructing efficient and low-cost electrocatalysts.[194] Flower-like HEA/MoS_2/MoP exhibited excellent HER and OER electrocatalytic performance. It showed a low overpotential of 230 mV at the current density of 10 mA cm^{-2} for OER and 148 mV for HER in alkaline electrolytes, respectively.[338] Ni_2P–MoS_2 HNSAs/CC sample as both anode and cathode for overall water splitting requires an impressively low onset potential of only 1.574 V to attain a current density of 10 mA cm^{-2} and displays excellent long-term stability. The facile synthesis method and insights into the HER and OER active interfaces reported here will advance the development of high-performance bifunctional overall water-splitting electrocatalysts. They can be used for both OER and HER.[339] Although research on TMP@MoS_2 heterostructures for the Oxygen Evolution Reaction (OER) is less extensive than for the Hydrogen Evolution Reaction (HER), existing studies demonstrate promising catalytic performance and stability. These findings highlight the potential of TMP@MoS_2-based materials as efficient and cost-effective bifunctional electrocatalysts for overall water splitting, paving the way for future advancements in sustainable energy conversion.

9. Comparative electrochemical performance of TMP@MoS_2 heterostructures

9.1 Comparison with metal phosphides/oxides/sulfides in electrocatalysts

Table 4 compares the HER and OER electrocatalytic activity for the TMP@MoS_2 heterostructure with that for the standard metal phosphides, metal oxides, and metal sulfides. The surface properties of the metal phosphides and the MoS_2 thus work in synergy to enhance their catalytic properties, as evidenced by lower overpotentials for HER and OER. It was found that MoP@MoS_2 demonstrated higher hydrogen evolution than MoP, while CoP@MoS_2 has the lowest overpotential among oxygen evolution catalysts compared to most of those where rGO supported CoP. Compared to most metal oxides, the TMP@MoS_2 heterostructure has lower cell voltage values for the water-splitting process and remains constant among all others. However, NiP/MoS_2 heterostructures exhibited high stability and distinctive capabilities, even under the most rigorous conditions. Therefore, TMP@MoS_2 heterostructure could become one of the best options for renewable energy applications. These hetero-crystals are prospective materials to boost HER, OER, and water-splitting processes. They are also critical potential substances from energy conversion and storage, particularly activity stability.

9.2 Comparison with metal phosphides/oxides/sulfides in supercapacitors

Table 5 shows the comparison, indicating that the electrode materials that form the TMP@MoS_2 heterostructures were much better when compared to those formed by metal phosphides, oxides, or sulfides. MoS_2 increases the electrochemical properties of the materials and enhances the specific capacitance, the cyclic stability, and the energy density.

For instance, NiCoP@MoS_2 delivered far superior capacitance performance than NiCoP. Researchers said the layer structure with MoS_2 was the primary contributing factor. Such a structure would promote active sites and electron transport to achieve the best electrochemical performance. Likewise, capacitance in ZnS/MoS_2/NF was enhanced since MoS_2 and system stability provided better energy storage and were also boosted.

The layer structure of MoS_2 forms a conductive network for efficient electron transfer throughout all the charge/discharge cycles without any structural changes. This thereby positions MoS_2 in the linear way of obtaining high-performance supercapacitors, opening up a new opportunity to advance energy storage technologies.

Table 4 Comparing TMP@MoS_2 heterostructures with metal phosphides/oxides/sulfides electrode materials in electrocatalysts

Catalyst	Substrate	Overpotential @10 mA cm^{-2} [mV]		Voltage for overall @10 mA cm^{-2} [V]	Tafel slope [mV dec^{-1}]		Stability	Electrolyte	Ref.
		η_{HER}	η_{OER}	V_m	HER	OER			
MoP/MoS_2	Ni foam	96 mV	—	1.98	48	—	—	1 M KOH and 1 M PBS	340
MoP	Ni foam	114	265	1.62	34.4	56.6	—	1 M KOH	341
$CoP@MoS_2$	CoCo-PBA	201	—	—	70.4	—	3000 cycles	0.5 M H_2SO_4	342
CoP	RGO	58	284	1.66	58.3	116.4	—	1 M KOH	343
Ni_2P/MoS_2	—	75	—	—	76	—	8 h	0.5 M H_2SO_4	344
Ni_2P	N-RGO	80	—	—	93.1	—	—	0.5 M H_2SO_4	345
$NiCoP/MoS_2$	Ni foam	148	—	—	109	—	Highly stable	1 M KOH	189
NiCoP	Ni foam	222	—	—	153	—	—	1 M KOH	189
MoS_2	Ni foam	181	—	—	—	—	—	1 M KOH	189
FeP/MoS_2	—	110	—	—	67.8	—	Good stability	0.5 M H_2SO_4	231
FeP	—	210	—	—	76.5	—	—	0.5 M H_2SO_4	231
$MoP_xS_y@NiFeP_xSy@NPS-C$	MoO_3	—	274	—	—	65.6	100 h	1 M KOH	346
MoS_2	—	265	—	—	86.2	—	—	0.5 M H_2SO_4	231
Co_3O_4/MoS_2	Nickel foam	205	230	—	98	45	10 h	1 M KOH	347
MoS_2–MoO_{3-x}/Ni_3S_2	Nickel foam	76	—	—	53.2	—	17 h	1 M KOH	348
CoS_2–MoS_2	Carbon cloth	60	240	1.52	86	68	24 h	1 M KOH	349
$MoO_2/MoS_2/MoP$	—	135	—	—	67	—	1000 cycles	0.5 M H_2SO_4	191
$MoO_2/MoS_2/MoP$	—	145	—	—	71	—	1000 cycles	1 M KOH	191
MoS_2/NiS_2	Carbon cloth	80	303	1.63	61	58	Excellent stability	Alkaline solution	350
MoS_2/MoO_2	—	157	—	—	119	—	Half-day	1 M KOH	351

Table 5 Comparing TMP@MoS_2 heterostructures with metal phosphides/oxides/sulfides electrode materials in supercapacitors

Metal phosphides	Capacitance ($F\ g^{-1}$)	Cycling stability (%)	Energy density ($W\ h\ kg^{-1}$)	Power density ($W\ kg^{-1}$)	Coulombic efficiency (%)	Ref.
MnP–MoS_2	432.3	86.2	16.7	403.9	93.4	190
NiCoP@MoS_2	2352.407	—	52	321	—	20
NiCoP	1279.2	—	45.5	124.2	—	352
CoP	447.5	96.7	19	350.8	—	353
FeP	149.11	41	2.02 mW h cm^{-3}	9.02 mW cm^{-3}	—	354
Cu_3P	300.9	81.9	44.6	0.017	—	355
Carbon@MoS_2/MoO_2	569	67.1	30.8	800	91.4	356
SnS_2/MoS_2	466.6	88.2	115	2230	—	357
TiO_2@MoS_2	337	Long cycle stability	—	—	—	358
MoS_2–RuO_2	719	100	35.92	0.6	—	359
CuO/MoS_2	268	90.02	26.66	1599.6	—	360
MoS_2/CeO_2	166.6	—	—	—	—	361
MnO_2 nanowire/MoS_2	212	84.1	29.5	1316	—	362
nanofibers/TiO_2@MoS_2	510.4	95.7	—	—	—	363
ZnS/MoS_2/NiF	3540	97	122	2500	100	364
MoS_2/NiF	1666	79	72	250	85	364
MoS_2–PbS	205.50	—	6.95	24.82	—	365
Core–shell $TiNb_2O_7$@MoS_2/C	—	93.7	147.2	2470.5	—	366
$MnCo_2O_4$@MoS_2	512	91.87	36	19	99.57	367

9.3 Comparison with metal phosphides/oxides/sulfides in batteries

This compares electrochemical performance among TMP@MoS_2 heterostructures with metal phosphides, oxides, and sulfides as electrode materials that differ significantly in discharge capacity, cycling performance, and rate capability. The first discharge capacity of MoP–MoS_2 heterostructure arrays was 1090.02 mA h g^{-1} at a mass loading of 3.9 mg cm^{-3}, with a corresponding efficiency that remained above 98% for no less than 1000 cycles—a much better result relative to the stand-alone MoP and MoS_2. They show much lower discharge capacities of 495 mA h g^{-1} and 436 mA h g^{-1}, respectively. This hybridization of MoS_2 with other metal compounds adds CoP–C@MoS_2/C and FeP@SnP@MoS_2 for enhanced discharge capacities of 1000 mA h g^{-1} and 905.3 mA h g^{-1}, respectively, showing the synergy between MoS_2 with metal phosphides and improved cycling stability. In comparison, other heterostructures, such as MoS_2–MoO and MoS_2–SnS, have even higher discharge capacities of 1531 mA h g^{-1} and 1504.6 mA h g^{-1}, respectively, further explaining the role of composite materials in enhancing battery performance. These materials have a high-rate capability and excellent cycling performance, ladling out the potential of TMP@MoS_2 heterostructures for promising candidates of next-

Table 6 Comparing metal phosphide/MoS_2 heterostructures with metal phosphides/oxides/sulfides electrode materials in batteries

Metal phosphides	Discharge capacity (mA h g^{-1})	Mass loading (mg cm^{-2})	Efficiency (%)	Cycling performance (mA h g^{-1})	Rate capability (mA h g^{-1}/A. g^{-1})	Ref.
MoP–MoS_2	1090.02	3.9	98	1000	—	12
MoP	495	1.0	—	—	—	368
MoS_2	436	—	—	187.48	—	369
CoP–C@MoS_2/C	1000	—	99.4	500	—	370
CoP	1866.9	—	80.3	635.3	656.81	371
Fe_2P@$SnP_{0.94}$@MoS_2	905.3	—	99.4	797.5	797.5	372
Fe_2P	413	—	—	—	396	373
Fe_7S_8–MoS_2	1250.5	6	—	1000.2	674.4	374
MoS_2–MoO_3	1531	5.9	92	640	—	375
CoS/NC@MoS_2	1417.2	0.566	74.82	1256.6	100	376
$NiCo_2S_4$@MoS_2	398	0.65	>99	400	398	377
MnS–MoS_2	1246.2	—	59.2	397.2	—	378
VS_4/MoS_2	1061.4	4.6	90	808.3	665.0	379
MoS_2–SnS	1504.6	3.50	—	1083.312	690.1	380
Sb_2S_3/MoS_2	701	—	95	561	—	381
MoS_2/FeS_2/C	613.1	1.1–1.5	100	77.2	574.6	382
G/NiS_2–MoS_2	509.6	1.2–1.6	>99	383.8	—	383
MoS_2/ZnS-NC	1427.2	2.4	93.7	760.15	—	384
MoS_2/WS_2	620	—	64	333	487	385
(1T-2H MoS_2)/CoS_2	729.6	—	99	300	400	386

generation energy storage devices, balanced against traditional metal phosphides, oxides, and sulfides (Table 6).

9.4 Comparative performance of TMP@MoS_2 across energy storage and catalysis

By directly comparing the relative performance of TMP@MoS_2 heterostructures in batteries, supercapacitors, and electrocatalysts based on Tables 2–4, it will be evident that every application has its peculiar benefits from these materials.[387] In batteries, TMP@MoS_2 heterostructures such as MoP–MoS_2 and Fe_7S_8–MoS_2 have very high discharge capacities while maintaining excellent cycling stability. For instance, MoP–MoS_2 at the end of 1000 cycles delivers a discharge capacity of 1090.02 mA h g^{-1} with an efficiency of 98%, which for Fe_7S_8–MoS_2 is further increased to 1250.5 mA h g^{-1}. These make the TMP@MoS_2 heterostructures uniquely suitable for long-term energy storage, wherein performance during thousands of charge–discharge cycles becomes significant. On the other hand, this TMP@MoS_2 heterostructure has significantly helped supercapacitors' capacitance and energy density. NiCoP@MoS_2 and ZnS/MoS_2/NiF are outstanding materials used in applications; between them, the capacitance of NiCoP@MoS_2 was somewhat exceptional in terms of its 2352.407 F g^{-1} at an energy density of 52 W h kg^{-1}. One beyond is the ZnS/MoS_2/NiF-type capacitor, which attains a capacitance value of 3540 F g^{-1} but tells a far greater cycling stability of 97 percent. These features further make TMP@MoS_2 heterostructures ideal for applications requiring high power density and rapid energy discharge. They are better candidates for developing supercapacitors for applications with fast charging and discharging cycles. For example, MoP/MoS_2 and CoS–MoS_2 heterostructures in TMP@MoS_2 substrates showed good catalytic performance, especially hydrogen evolution reactions. In a separate study, MoS_2/MoS_2 heterostructures demonstrated an overpotential of only 96 mV for HER, suggesting a highly catalytically efficient material. CoS–MoS_2 further reduced it to 60 mV, thus being highly stable and efficient as an electrocatalyst. With such properties, the TMP@MoS_2 heterostructures will work out the most in low-overpotential, strongly stable energy–conversion processes. Supercapacitors have demonstrated the most dramatic rise in performance among all investigated devices. However, which application can exploit the advantages of TMP@MoS_2 heterostructures "best" depends on specific requirements. Provided that long-term energy storage is required, batteries equipped with electrodes configured from TMP@MoS_2 heterostructures offer both large discharge capacity and stability of operation. In the case when fast energy delivery is required, the performance of supercapacitors is unmatched. On the other hand, electrocatalysts both derive an enhanced catalytic efficiency and durability related to energy conversion. Though all three applications have some compelling reasons, TMP@MoS_2 heterostructures have the most significant advantages when applied for supercapacitors.

This comparative analysis is represented by a figure that shows the different electrochemical performances of TMP@MoS_2 heterostructures in various fields, including electrocatalysis, supercapacitors, and batteries. Specifically, in electrocatalysis, this is

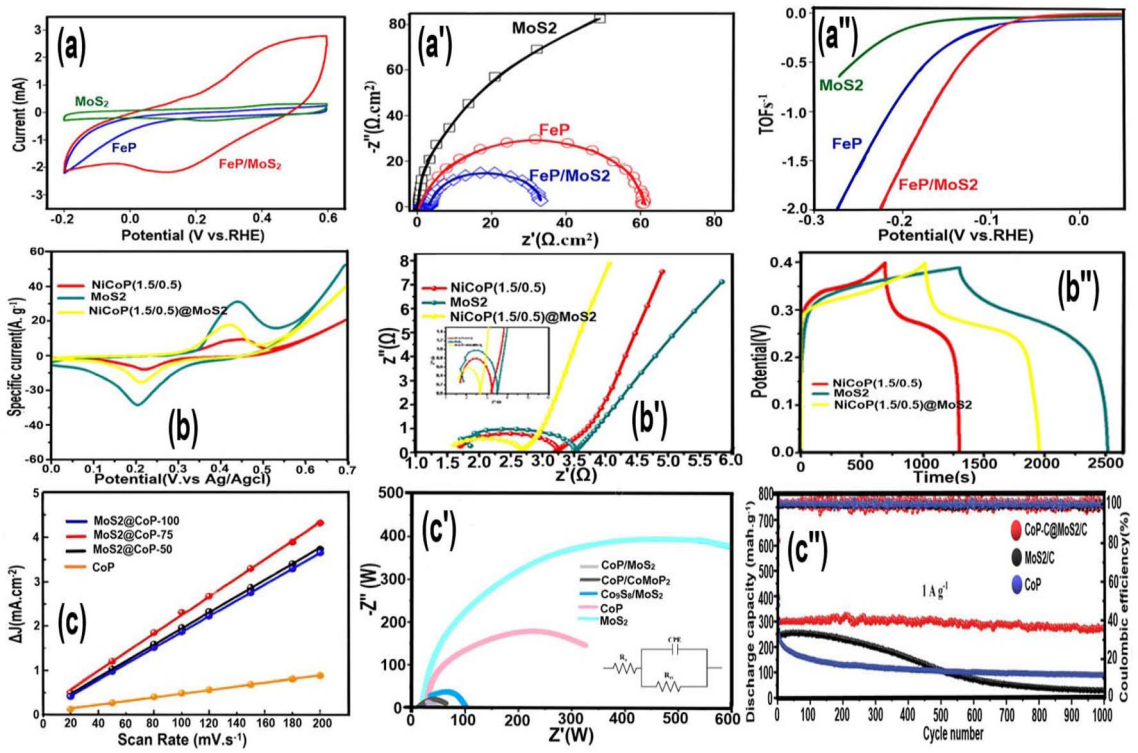

Fig. 12 Comparative analysis of the electrochemical performance of various TMP@MoS_2 (a–a″, b–b″ and c–c″) electrocatalyst. Reproduced from ref. 232 with permission from [American Chemical Society].

manifested as the FeP/MoS_2 composite standing superior to pure MoS_2 and FeP in both current density and Tafel slope for HER, as shown in Fig. 12a–a″. Specifically, the electrochemical impedance spectroscopy result from Fig. 12a′ shows that FeP/MoS_2 has the lowest charge transfer resistance compared to other counterparts. This would indicate that electron transfer was more efficient during catalytic processes. The TOF curves in Fig. 12a″ confirm that the intrinsic catalytic activity of FeP/MoS_2 is the highest among all those materials tested. This NiCoP@MoS_2 heterostructure performed very well for supercapacitors concerning specific capacitance and cycling stability, as shown in Fig. 12a–a″ to b–b″. Obviously, from Fig. 12b, the NiCoP@MoS_2 has much higher specific current and electrochemical reversibility than pure MoS_2, according to the CV curves. From the EIS plot in Fig. 12b′, these composite exhibits much lower resistance for NiCoP@MoS_2; that is, more rapid charge/discharge cycles. Fig. 12b″ illustrates the excellent cycling stability for NiCoP@MoS_2. It was found to retain, even at a large number of cycles, a pretty large capacitance compared with that for MoS_2 or the pristine NiCoP material. Regarding batteries, the CoP@MoS_2 composite represented in Fig. 12c to c″ delivers a distinguished large discharge capacity and long-term cycling stability. Concretely, as shown in Fig. 12c, differential capacity *versus* scan rate curves are presented; here, CoP@MoS_2 has higher capacity retention and better rate capability than MoS_2 and pure CoP. This is further supported by the Nyquist plot in Fig. 12c′, where CoP@MoS_2 has lower resistance, thus contributing to its better electrochemical performance. Fig. 12c″ outlines the outstanding cycling stability and coulombic efficiency of CoP@MoS_2, during which a high discharge capacity can be maintained for more than 1000 cycles, far superior to that of MoS_2 and CoP alone. The components of TMP@MoS_2 2D heterostructures have distinctly improved electrochemical performance, specifically FeP/MoS_2 for electrocatalysis, NiCoP@MoS_2 for supercapacitors, and CoP@MoS_2 for batteries. Each composite material has characteristics superior to the others in its way. Still, it tailors to the requirements or needs that an application would need, making TMP@MoS_2 heterostructures quite versatile and very practical in energy storage and conversion.

Indeed, TMP@MoS_2 heterostructures have shown unparalleled versatility and performance in various applications, including electrocatalysis, supercapacitors, and batteries.[12,20,388] Their high catalytic activity in electrocatalysis reflects reduced overpotentials for HER and OER reactions.[389] Moreover, superior specific capacitances and energy density can be achieved in supercapacitors,[20] and batteries will have high discharge capacities and long-term stability during cycling.[332] This ensures the prospect of promising candidacy in next-generation energy technology. Nevertheless, the following limitations and challenges somewhat offset these strengths and require further research and optimization.

10. Challenges and future perspectives in TMP@MoS_2 research

10.1 Limitations in electrocatalysis

CoP@MoS_2 heterostructure is susceptible to instability in equilibrium between MoS_2 and CoP phases unless it is optimally engineered. If external MoS_2 layers are too thin, there is a lack of sufficient CoP to activate surface inertness and reduce charge and mass conductivity.[15] If there is excessive CoP, layered architecture is destabilized. While multiple studies have explored CoP/MoS_{22} heterojunctions as hydrogen evolution catalysts, a scalable and high-performance synthesis approach remains an open research question. Consequently, much work is still needed to develop efficient, cost-effective, and highly durable CoP@MoS_2 catalysts for HER.[390] During hydrogen evolution, gas bubbles can accumulate on the heterostructure's surface, blocking active sites and lowering efficiency.[391] Even though heterojunction catalysts promise superior catalytic properties compared to monocomponent systems, they often suffer from low stability, weak adhesion to electrodes, and aggregation of active chemicals, which limit their exposure to catalytic sites. The incorporation of strong interfacial bonding, defect engineering, and encapsulation in conductive matrices can improve catalyst durability and efficiency.[392]

10.2 Limitations in supercapacitors

Transition metal phosphides can also show lower inherent electrical conductivity than materials based on carbon, such as graphene and carbon nanotubes, reducing charge mobility and lower power density in supercapacitors.[393] Electrolyte selection is also crucial as some TMPs can degrade with some electrolytes and cause a drop in efficiency. Surface modifications and protective coatings can reduce this by optimizing electrode/electrolyte compatibility.[394] Supercapacitor energy density is directly proportional to capacitance and operating voltage range and is still lower for many existing supercapacitors compared to batteries even with high-power-density active electrodes. Hence, merely combining TMPs and MoS_2 would not increase energy density significantly unless heterostructure engineering is finely optimized to enhance charge storage mechanisms.[274] Further, TMP-MoS_2 heterostructure synthesis is still complex and requires stringent conditions and higher temperature and is difficult to industrially scale. Future work would be to design simpler and scalable synthesis methods such as rapid chemical vapor deposition or template-assisted hydrothermal methods.[314]

10.3 Limitations in batteries

The optimal electrochemical performance in MoS_2/MoP Mott–Schottky heterostructures in lithium–sulfur batteries is achieved when MoS_2 and MoP are in the proper ratio.[332] The excess phosphorus in phosphides ($x : y < 1$) is detrimental to electrical conductivity and reduces them to be less efficient in electronics and batteries. An increased amount of phosphorus also reduces structural stability and leads them to decompose on thermal treatment. This trade-off points towards the need for controlling composition with precision in TMP@MoS_2 heterostructures. With a reduced Ni : P ratio, metal–metal interactions are minimized and with them, conductivity and catalytic efficiency too diminish. Doping techniques and hybrid structures with conductive additives would overcome these limitations.[232]

TMP@MoS_2 heterostructures are of great potential as a material class based on structural stability, electrical

conductance, and large specific capacity.[20] They will be promising candidates for improving critical energy storage and electrocatalysis.[395] These heterostructures can significantly enhance catalytic activity by leveraging synergistic properties between TMPs and MoS_2.[392]

While TMPs have demonstrated intrinsic catalytic performance in HER and OER, their long-term durability in real-world applications remains insufficient.[396] Introducing MoS_2 into TMP-based catalysts reduces overpotential, improves electron transport, and exposes additional active sites;[15] for instance, CoP@MoS_2 heterostructures exhibit a reduced overpotential of 60 mV in HER, attributed to electronic modulation induced by MoS_2.

TMP@MoS_2 heterostructures offer high performance in energy storage applications at both high-power densities and long-term cycling conditions. Incorporating MoS_2 into TMP-based materials in batteries enhances cycling stability and discharge capacity compared to their individual components.[370,397] MoP@MoS_2,[12] for example, delivers a discharge capacity of 1090.02 mA h g^{-1} with 98% efficiency after 1000 cycles, making it one of the most durable electrode materials for advanced energy storage systems. This improvement arises from the rapid ion transport facilitated by the layered MoS_2 structure, enabling enhanced charge–discharge cycling. Similarly, NiCoP@MoS_2 has demonstrated a specific capacitance of 2352.4 F g^{-1} and an energy density of ~52 W h kg^{-1}, outperforming conventional electrode materials and positioning it as a top candidate for high-performance energy storage applications.[20]

Beyond their outstanding performance, TMP@MoS_2 heterostructures offer industrial scalability and cost-efficiency solutions. Hydrothermal synthesis[15] and chemical vapor deposition[398] provide scalable methods for producing high-purity TMP@MoS_2 heterostructures, allowing precise control over particle morphology and size. These methods enable cost-effective large-scale production, making TMP@MoS_2 materials feasible for commercial applications. However, challenges remain.[399] Synthesis methodologies must be further optimized for large-scale production without sacrificing material quality.[400] The stability and efficiency of TMP@MoS_2 for HER and OER can be further enhanced by fine-tuning reaction conditions, improving interfacial engineering, and developing innovative composite structures. Further synthesis and integration techniques refinement is necessary to fully realize TMP@MoS_2's potential in practical energy applications.

Overcoming these research and industry challenges will allow TMP@MoS_2 heterostructures to revolutionize energy storage and electrocatalysis. Their development aligns with global sustainability goals, contributing to efficient and environmentally friendly energy solutions. By integrating green synthesis techniques, optimizing charge transport, and improving catalytic durability, TMP@MoS_2 heterostructures could become the key materials for next-generation energy technologies.

10.4 Effect of size, stability, and other compositions

The structural stability, composition, and size of transition metal phosphide/molybdenum disulfide (TMP@MoS_2) heterostructures are responsible for regulating their electrochemical energy storage behavior.[401–404] Nanoscale reduction promotes electrochemically active sites, ion diffusion, and charge transfer, leading to structural instability and agglomeration; therefore, there is a requirement for optimal balance.[405–407]

Stability has been enhanced using such methods as heteroatomic doping,[408] hybridization with a conductive matrix,[409] and coating with carbon.[410]

Compositions are crucial in controlling catalytic activity, charge storage, and electronic properties.[411,412] Different transition metals (Ni, Co, Fe, Mn) offer different electronic structures and redox behaviors.[413] Bimetallic/ternary phosphides (such as Ni–Co–P and Fe–Co–P) offer synergistic effects with improved conductivity and redox capability.[414] Integrating materials such as graphene, MXenes, or MOFs to further improve electrode properties and multi-functionalities.[415]

Modulating these structural factors allows the rational design of heterostructures that exhibit higher energy density as well as improved cycling stability and kinetic behavior for charge storage, and TMP@MoS_2 represents a promising material for next-generation batteries and supercapacitors.

10.5 Strategies for overcoming challenges in TMP@MoS_2 heterostructures for energy storage applications

The progress in the development of the TMP@MoS_2 heterostructures for energy storage devices has been hindered by several issues, such as low interface stability,[416] low efficiency in the transfer of charges,[94] and scalability problems[417] in the fabrication process. To encounter these bottlenecks, interface engineering,[418] atomic-scale design,[419] doping,[408,420] surface modification,[421] and multifunctional design methodologies[422] are being addressed from the perspective of science.

10.5.1 Interface engineering and atomic-scale design. The interfacial contact between TMPs and MoS_2 is crucial for the activity of TMP@MoS_2 heterostructures.[423] Low interfacial contact leads to resistance and poor transportation of charges.[424] Atomic-level processing techniques such as epitaxial growth and heterojunction optimization are required to increase interfacial bonding and minimize resistance.[425] Strong chemical bonding and good van der Waals interactions in the interface were found to increase electron mobility and electrochemistry by a large margin.[426]

10.5.2 Doping and surface modification approaches. Doping has been extensively employed to modify MoS_2 electronic band structure and increase conductivity.[427] Nitrogen, boron, and phosphorus heteroatom doping have been found to enhance electrochemical activity by offering active sites for kinetic reactions and storage.[428] Further, the low electrical conductivity and structural instability issues with MoS_2 have also been addressed using surface modification techniques,[429] which include functionalization with carbonaceous species or conducting polymers (*e.g.*, CNT, graphene).[430]

10.5.3 Advanced fabrication and scaling techniques. Scalability remains a challenge in the preparative synthesis of TMP@MoS_2 heterostructures.[431] Classical wet chemical

synthesis methods, although efficient, are plagued by inhomogeneous morphology and variability across different batches.[432] CVD (chemical vapor deposition), atomic layer deposition (ALD), and laser-based methods are sophisticated methods that have been explored to offer control of thickness with accuracy and homogeneous material dispersion on a large scale.[433–435] High surface area and better ion access and stability can be achieved through self-assembly processes to form heterostructures.[436]

10.5.4 Design of multifunctional TMP@MoS_2 heterostructures. To further improve the electrochemical practicality of TMP@MoS_2 nanostructures, researchers have tailored multifunctional heterostructures with synergistic attributes that are proven to cater to the performance of supercapacitors and batteries.[437] For example, it has been reported that hierarchical pore structures with optimized ion channel size for diffusion significantly affect the electrochemical activity.[438] Energy storage and catalytic properties of hybrid structures are also investigated as future-generation energy storage materials.[439]

10.6 Recent advances in TMP@MoS_2-based electrochemical energy storage

Recent advancements in the area of TMP@MoS_2-based electrochemical energy storage reveal the potential that these heterostructures have for batteries and supercapacitors. Studies have established that the coupling between the transition metal phosphides (TMPs) and the MoS_2 enhances the storage of charges through the increase in the number of active sites as well as electron transfer. Particularly, self-assembly Cu–Mo sulfide and phosphide compounds possess high capacitance and stability with up to 86.9% retention of their initial capacity when cycled to as many as 4000 cycles. Ternary TMPs and sulfides also possess higher conductivity, facilitating multi-electron redox reactions and hence enhancing the energy density when utilized in the case of supercapacitors.

MoS_2-based heterostructures also hold promise in hydrogen evolution reactions (HER). A hierarchical CoP/Ni_2P/MoS_2 catalyst exhibits outstanding catalytic activity in the presence of neutral, alkaline, as well as acidic media, with the advantage of optimized charge transfer and structural design. In addition, Mo-based compounds, such as phosphides, oxides, and carbides, are instrumental in the development of lithium–sulfur (Li–S) batteries through conductivity, stabilization of the polysulfides, and enhanced electrochemical properties. Despite the progress, more work has to be done to make these materials suitable for commercial applications on a large scale.[13,440,441] Metal phosphides are shown to be promising for enhancing the performance of lithium–sulfur batteries (LSBs) by addressing significant issues, including the lithium polysulfide (LiPS) shuttle effect, sluggish sulfur conversion, and growth of lithium dendrites. Their high catalytic activity and tunable cationic character make them active in LiPS adsorption and rapid conversion, promoting sulfur utilization and battery stability. Additionally, their addition to composite materials enhances catalytic efficiency, whereas their application in separator modification and the coating of the lithium anode further increases battery efficiency. Despite the continued issues with conductivity and uniform deposition of lithium, continued developments in metal phosphide design are contributing towards the commercialization of high-performance LSBs.[442]

Artificial Intelligence (AI) is now a potent tool to expedite the discovery,[443] optimization, and design of heterostructure materials for energy storage[444] by circumventing time and resource-consuming traditional computational and experimental methods.[445–447] AI-enabled methods like machine learning (ML), deep learning (DL), and high-throughput computational modeling enable efficient exploration of large chemical and structural spaces.[448–450] AI methods screen large databases to provide predictions for optimal compositions,[451] crystal structures,[452] and interfacial interactions in TMP@MoS_2 heterostructures[453] and shorten material discovery time by orders of magnitude.[454] AI-powered molecular dynamics (MD) simulations and neural network-based interatomic potentials optimize interface stability[455,456] and defect engineering[455] and enhance catalytic activity and charge transfer behavior.[457] AI-enabled robotic synthesis platforms and high-throughput experiments speed up heterostructure development by identifying optimal synthesis conditions for scalable manufacturing.[458,459] AI models based on electrochemical test data also predict long-term stability,[460] energy density,[461] and rate capability in batteries and supercapacitors[462] and optimize electrode architectures and ion diffusion pathway simulations to maximize device efficiency.[463,464]

11. Conclusion

This research highlights the promise of TMP@MoS_2 heterostructures to function as next-generation materials in electrocatalysis and energy storage in electrochemistry. The high conductance and catalytic activity of transition metal phosphides and catalytic efficiency and structure stability of molybdenum disulfide make such heterostructures promising next-generation batteries, supercapacitors, and electrocatalytic applications like HER and OER. The synergy between TMP and MoS_2 enhances charge transfer, stability, and exposure of active sites and addresses some of the primary issues with present energy storage technology. Despite such advantages, challenges still persist with regard to optimizing the scalability of synthesis, long-term stability, and application viability at a large scale. Future research will be needed to enhance synthesis techniques, interfacial engineering, and compositional tuning with new methodologies to boost performance. Further research in such areas will be critical to unlocking the full capability of TMP@MoS_2 in applications involving sustainable energy.

Data availability

No primary research results, software or code have been included and no new data were generated or analysed as part of this review.

Conflicts of interest

There are no conflicts to declare.

Acknowledgements

This work was supported by the Iranian Research & Development Center for Chemical Industries (IRDCI), and Pharmaceutical Analysis Research Center, Tabriz University of Medical Sciences, Tabriz, Iran [76636].

References

1 J. L. Holechek, H. M. Geli, M. N. Sawalhah and R. Valdez, *Sustainability*, 2022, **14**, 4792.
2 E. Jamshidi, S. Dalvand, F. Manteghi and S. M. Mousavi Khoshdel, *iScience*, 2025, 111672.
3 S. A. Mousavianfard, A. Molaei, M. Manouchehri, A. Foroozandeh, A. Shahmohammadi and S. Dalvand, *J. Energy Storage*, 2025, **109**, 115232.
4 A. D. A. Bin Abu Sofian, H. R. Lim, H. Siti Halimatul Munawaroh, Z. Ma, K. W. Chew and P. L. Show, *Sustainable Dev.*, 2024, **32**, 3953.
5 R. T. Yadlapalli, R. R. Alla, R. Kandipati and A. Kotapati, *J. Energy Storage*, 2022, **49**, 104194.
6 Z. Zhu, T. Jiang, M. Ali, Y. Meng, Y. Jin, Y. Cui and W. Chen, *Chem. Rev.*, 2022, **122**, 16610.
7 T. S. Babu, K. R. Vasudevan, V. K. Ramachandaramurthy, S. B. Sani, S. Chemud and R. M. Lajim, *IEEE Access*, 2020, **8**, 148702.
8 S. Dalvand, A. Foroozandeh, A. Heydarian, F. S. Nasab, M. Omidvar, N. Yazdanfar and A. Asghari, *Ionics*, 2024, **30**, 1857.
9 Y. Li, J. Zhang, Q. Chen, X. Xia and M. Chen, *Adv. Mater.*, 2021, **33**, 2100855.
10 S. M. Qashqay, J. Rahimi, M.-R. Zamani-Meymian and A. Maleki, *J. Energy Storage*, 2023, **72**, 108548.
11 R. Eivazzadeh-Keihan, R. Taheri-Ledari, N. Khosropour, S. Dalvand, A. Maleki, S. M. Mousavi-Khoshdel and H. Sohrabi, *Colloids Surf., A*, 2020, **587**, 124335.
12 X. Wang, N. Deng, J. Ju, G. Wang, L. Wei, H. Gao, B. Cheng and W. Kang, *J. Membr. Sci.*, 2022, **642**, 120003.
13 X. Cheng and Y. Tong, *ACS Appl. Energy Mater.*, 2023, **6**, 9577.
14 M. Afshari Babazad, A. Foroozandeh, M. Abdouss, H. SalarAmoli, R. A. Babazad and M. Hasanzadeh, *TrAC, Trends Anal. Chem.*, 2024, **180**, 117964.
15 T. Xia, L. Zhou, S. Gu, H. Gao, X. Ren, S. Li, R. Wang and H. Guo, *Mater. Des.*, 2021, **211**, 110165.
16 X. Wang, G. Zhang, B. Wang, Y. Wu and S. Guo, *ACS Sustain. Chem. Eng.*, 2024, **12**, 14018.
17 A. Foroozandeh, M. Abdouss, H. SalarAmoli, M. Pourmadadi and F. Yazdian, *Process Biochem.*, 2023, **127**, 82.
18 J. Zhang, J. Ma, R. Cui, W. Ling, M. Hong and R. Sun, *Chem. Eng. J.*, 2025, **503**, 158427.
19 A. Foroozandeh, H. SalarAmoli, M. Abdouss and M. Pourmadadi, *Sens. Actuators Rep.*, 2024, **7**, 100195.
20 A. Shahmohammadi, S. Dalvand and H. Baheri, *Mater. Chem. Phys.*, 2024, **317**, 129150.
21 F. Khoramjah, M. Omidvar, M. S. Miresmaieli, S. Dalvand, A. Asghari, M. Kambarani and N. Mohammadi, *Diamond Relat. Mater.*, 2023, **132**, 109590.
22 S. S. Mirzaei, M. Pourmadadi, A. Foroozandeh, A. A. Moghaddam, M. Soltani, N. Basirhaghighi and M. Ahmadi, *J. Appl. Electrochem.*, 2024, **54**, 1887–1900.
23 X. Peng, Y. Lv and S. Zhao, *Coatings*, 2022, **12**, 68.
24 S. Ghorai and A. Govind Rajan, *Chem. Mater.*, 2024, **36**, 2698.
25 W. Fu, M. John, T. D. Maddumapatabandi, F. Bussolotti, Y. S. Yau, M. Lin and K. E. Johnson Goh, *ACS Nano*, 2023, **17**, 16348.
26 M. Omidvar, S. Dalvand, A. Asghari, N. Yazdanfar, H. Y. Sadat and N. Mohammadi, *Fuel*, 2023, **347**, 128472.
27 Y. Zhu, T.-R. Kuo, Y.-H. Li, M.-Y. Qi, G. Chen, J. Wang, Y.-J. Xu and H. M. Chen, *Energy Environ. Sci.*, 2021, **14**, 1928.
28 R. Eivazzadeh-Keihan, R. Taheri-Ledari, M. S. Mehrabad, S. Dalvand, H. Sohrabi, A. Maleki, S. M. Mousavi-Khoshdel and A. E. Shalan, *Energy Fuels*, 2021, **35**, 10869.
29 Z. Sadat, R. Eivazzadeh-Keihan, V. Daneshvari-Esfahlan, S. Dalvand, A. Kashtiaray and A. Maleki, *Sci. Rep.*, 2024, **14**, 3137.
30 J. Dai, Y. Lv, J. Zhang, D. Zhang, H. Xie, C. Guo, A. Zhu, Y. Xu, M. Fan and C. Yuan, *J. Colloid Interface Sci.*, 2021, **590**, 591.
31 A. Asghari, S. Dalvand, M. sadat Miresmaeili, F. Khoramjah, M. Omidvar, M. Kambarani and N. Mohammadi, *Int. J. Hydrogen Energy*, 2023, **48**, 9776.
32 M. Yousaf, U. Naseer, Y. Li, Z. Ali, N. Mahmood, L. Wang, P. Gao and S. Guo, *Energy Environ. Sci.*, 2021, **14**, 2670.
33 P. Zhang, Y. Zhao, Y. Li, N. Li, S. R. P. Silva, G. Shao and P. Zhang, *Advanced Science*, 2023, **10**, 2206786.
34 S. Dalvand, M. Omidvar, A. Asghari, N. Mohammadi and N. Yazdanfar, *J. Porous Mater.*, 2023, **30**, 2069.
35 M. J. Kim, I. H. Choi, S. C. Jo, B. G. Kim, Y. C. Ha, S. M. Lee, S. Kang, K. J. Baeg and J. W. Park, *Small Methods*, 2021, **5**, 2100793.
36 S. Dalvand, Z. Khoushab, S. M. Mousavi-Khoshdel, H. Ghafuri, H. R. Esmaili Zand and M. Omidvar, Tungstate-Modified Ionic Liquid Functionalized Magnetic Graphene Oxide: Synthesis and Application as a High-Performance Supercapacitor, *SSRN*, 2021, preprint, DOI: 10.2139/ssrn.3968871.
37 J. Joy, A. Krishnamoorthy, A. Tanna, V. Kamathe, R. Nagar and S. Srinivasan, *Appl. Sci.*, 2022, **12**, 9312.
38 C. C. Piras, S. Fernández-Prieto and W. M. De Borggraeve, *Nanoscale Adv.*, 2019, **1**, 937.
39 L. K. Wei, S. Z. Abd Rahim, M. M. Al Bakri Abdullah, A. T. M. Yin, M. F. Ghazali, M. F. Omar, O. Nemes, A. V. Sandu, P. Vizureanu and A. E.-h. Abdellah, *Materials*, 2023, **16**, 4635.
40 W. Li, Y. Li, J.-H. Wang, S. Huang, A. Chen, L. Yang, J. Chen, L. He, W. K. Pang and L. Thomsen, *Energy Environ. Sci.*, 2024, **17**(15), 5387–5398.
41 S. A. Getaneh, A. G. Temam, A. C. Nwanya, P. M. Ejikeme and F. I. Ezema, *Mater. Sci. Technol.*, 2024, **40**, 185.

42 S. N. Alam, G. Arka, S. Nityananda, S. Pankaj, S. Kakara and A. M. Shafdar, *Consolidation of Mechanically Alloyed Powders*, Elsevier., 2024, pp. 119.
43 S. Arya, A. Singh, A. Ahmed, B. Padha, A. Banotra, U. Parihar, A. K. Sundramoorthy, S. Dixit and N. I. Vatin, *J. Energy Chem.*, 2025, **122**(23), 17155–17239.
44 H. Patil, S. K. Vemula, S. Narala, P. Lakkala, S. R. Munnangi, N. Narala, M. O. Jara, R. O. Williams III, H. Terefe and M. A. Repka, *AAPS PharmSciTech*, 2024, **25**, 37.
45 A. Singh, S. S. Shah, A. Dubey, A. Ahmed, S. V. Ranganayakulu, A. K. Sundramoorthy and S. Arya, *J. Energy Storage*, 2025, **109**, 115183.
46 D. Chen, B. Liu, G. Sun, W. Xu, Y. Zhu, Y. An, L. Zhu, X. Ding, J. Zhang and X. Lu, *Adv. Powder Technol.*, 2024, **35**, 104377.
47 O. S. ODEBIYI, G. Yuning, D. Hao, L. Biao and W. Shaona, *Mater. Chem. Phys.*, 2024, 129697.
48 P. Gao, X. Fan, D. Sun, G. Zeng, Q. Wang and Q. Wang, *Water*, 2024, **16**, 1639.
49 A. Ahmed, Y.-L. Chu, S.-J. Young, M. P. Chavhan, A. K. Sundramoorthy and S. Arya, *Ionics*, 2025, 1.
50 S. Verma, B. Padha, A. Ahmed, R. Singh, D. P. Dubal and S. Arya, *Prog. Energy*, 2024, **6**, 042002.
51 Z. Kong, Z. Wang, B. Chen, Y. Li and R. Li, *Materials*, 2023, **16**, 5763.
52 N. A. Mala, A. Singh, S. Bashir, A. Ghosh, A. Padder, S. Arya, N. Thakur, L. Guganathan and R. N. Ali, *Inorg. Chem. Commun.*, 2025, **174**, 113969.
53 H. Ismail, H. Mohamad and R. Hussin, *Emerging Advances in Integrated Technology, Universiti Tun Hussein Onn Malaysia Publisher's Office*, 2022, **3**, 9–14.
54 C. Real and F. J. Gotor, *Heliyon*, 2019, **5**, e01227.
55 F. J. Gotor, M. Achimovicova, C. Real and P. Balaz, *Powder Technol.*, 2013, **233**, 1.
56 Z. Wu, Y. Liang, E. Fu, J. Du, P. Wang, Y. Fan and Y. Zhao, *Metals*, 2018, **8**, 281.
57 A. Foroozandeh, M. A. Babazad, S. Jouybar, M. Abdouss, H. Salar Amoli, K. Dashtian and M. Hasanzadeh, *TrAC, Trends Anal. Chem.*, 2025, **183**, 118119.
58 L. L. Driscoll, E. H. Driscoll, B. Dong, F. N. Sayed, J. N. Wilson, C. A. O'Keefe, D. J. Gardner, C. P. Grey, P. K. Allan, A. A. L. Michalchuk and P. R. Slater, *Energy Environ. Sci.*, 2023, **16**, 5196.
59 L. M. Martínez, J. Cruz-Angeles, M. Vázquez-Dávila, E. Martínez, P. Cabada, C. Navarrete-Bernal and F. Cortez, *Pharmaceutics*, 2022, **14**, 2003.
60 S. Azzaza, S. Alleg and J. J. Suñol, *Adv. Mater. Phys. Chem.*, 2013, **03**, 90.
61 P. Pattanayak, S. Saha, T. Chatterjee and B. C. Ranu, *Chem. Commun.*, 2024, **61**, 247.
62 F. Shi and W. Xie, *Miner. Eng.*, 2016, **86**, 66.
63 S. Dalvand, Z. Khoushab, S. M. Mousavi-Khoshdel, H. Ghafuri, H. R. E. Zand and M. Omidvar, *Int. J. Hydrogen Energy*, 2023, **48**, 10098.
64 S. Reichle and M. Felderhoff, *Mechanochemistry and Emerging Technologies for Sustainable Chemical Manufacturing*, 2023, p. 151.
65 J. F. Reynes, V. Isoni and F. García, *Angew. Chem., Int. Ed.*, 2023, **62**, e202300819.
66 H. Chen, Q. Cao, Z. Ye, B. Lai, Y. Zhang, H. Dong, D. E. Crawford, O. M. Istrate and S. L. James, *Adv. Mater. Technol.*, 2024, **9**, 2301780.
67 M. Dhaval, S. Sharma, K. Dudhat and J. Chavda, *J. Pharmaceut. Innovat.*, 2022, **17**, 294.
68 J. N. Tiwari, K. Kumar, M. Safarkhani, M. Umer, A. T. E. Vilian, A. Beloqui, G. Bhaskaran, Y. S. Huh and Y.-K. Han, *Advanced Science*, 2024, **11**, 2403197.
69 R. Breitwieser, U. Acevedo Salas, S. Merah and R. Valenzuela, *Ferrite Nanostructures Consolidated by Spark Plasma Sintering (SPS)*, 2017.
70 A. Saberi, M. Kouhjani, D. Yari, A. Jahani, K. Asare-Addo, H. Kamali and A. Nokhodchi, *J. Drug Delivery Sci. Technol.*, 2023, **86**, 104746.
71 U. Nandi, V. Trivedi, S. A. Ross and D. Douroumis, *Pharmaceutics*, 2021, **13**, 624.
72 P. Evon, V. Vandenbossche, L. Candy, P.-Y. Pontalier and A. Rouilly, *Twin-screw Extrusion: A Key Technology for the Biorefinery*, ACS Publications, 2018, pp. 25.
73 L. Chai, S. Liu, S. Pei and C. Wang, *Chem. Eng. J.*, 2021, **420**, 129686.
74 M. B. Lopez and J. Ustarroz, *Curr. Opin. Electrochem.*, 2021, **27**, 100688.
75 C. C. Weng, J. T. Ren and Z. Y. Yuan, *ChemSusChem*, 2020, **13**, 3357.
76 T. Sivaranjani, T. Revathy and A. Stephen, *Controlled Electrochemical Deposition for Materials Synthesis*, CRC Press. 2020, pp. 25.
77 S. Islam, M. M. Mia, S. S. Shah, S. Naher, M. N. Shaikh, M. A. Aziz and A. S. Ahammad, *Chem. Rec.*, 2022, **22**, e202200013.
78 U. Mohanty, B. Tripathy, P. Singh, A. Keshavarz and S. Iglauer, *J. Appl. Electrochem.*, 2019, **49**, 847.
79 S. A. Lee, J. W. Yang, S. Choi and H. W. Jang, *Exploration*, 2021, **1**, 20210012.
80 F. C. Walsh, S. Wang and N. Zhou, *Curr. Opin. Electrochem.*, 2020, **20**, 8.
81 R. H. Miller, S. Hu, S. J. Weamie, S. A. Naame and D. G. Kiazolu, *J. Chem. Eng. Mater. Sci.*, 2021, **9**, 68.
82 J. Pu, Z. Shen, C. Zhong, Q. Zhou, J. Liu, J. Zhu and H. Zhang, *Adv. Mater.*, 2020, **32**, 1903808.
83 V. S. Saji, *J. Ind. Eng. Chem.*, 2019, **75**, 20.
84 S. Rajoria, M. Vashishtha and V. K. Sangal, *Environ. Sci. Pollut. Res.*, 2022, **29**, 72196.
85 J. Kim, H. Kim, G. H. Han, S. Hong, J. Park, J. Bang, S. Y. Kim and S. H. Ahn, *Electrodeposition: an Efficient Method to Fabricate Self-supported Electrodes for Electrochemical Energy Conversion Systems*, Wiley Online Library, 2022, p. 20210077.
86 F. Li, Y. Feng, Z. Li, C. Ma, J. Qu, X. Wu, D. Li, X. Zhang, T. Yang and Y. He, *Adv. Mater.*, 2019, **31**, 1901351.
87 B. K. Chakrabarti, M. Gençten, G. Bree, A. H. Dao, D. Mandler and C. T. J. Low, *Int. J. Energy Res.*, 2022, **46**, 13205.

88 I. Brandt, C. Araujo, V. Stenger, R. Delatorre and A. Pasa, *ECS Trans.*, 2008, **14**, 413.
89 S. A. Kumar, S. Sahoo, G. K. Laxminarayana and C. S. Rout, *Small*, 2024, **20**, 2402087.
90 S. Ji, J. Yang, J. Cao, X. Zhao, M. A. Mohammed, P. He, R. A. Dryfe and I. A. Kinloch, *ACS Appl. Mater. Interfaces*, 2020, **12**, 13386.
91 J. Theerthagiri, A. P. Murthy, S. J. Lee, K. Karuppasamy, S. R. Arumugam, Y. Yu, M. M. Hanafiah, H.-S. Kim, V. Mittal and M. Y. Choi, *Ceram. Int.*, 2021, **47**, 4404.
92 S. Kang, C. Wang, J. Chen, T. Meng and J. E, *J. Energy Storage*, 2023, **67**, 107515.
93 R. I. Walton, *Chem.–Eur. J.*, 2020, **26**, 9041.
94 A. Ray, S. Sultana, L. Paramanik and K. Parida, *J. Mater. Chem. A*, 2020, **8**, 19196.
95 Z. Li, J. Yang, T. Guang, B. Fan, K. Zhu and X. Wang, *Small Methods*, 2021, **5**, 2100193.
96 A. H. Mamaghani, F. Haghighat and C.-S. Lee, *Chemosphere*, 2019, **219**, 804.
97 R. Tyagi, O. Ruzimuradov and J. Prakash, *Mater. Chem. Phys.*, 2023, **307**, 128108.
98 L. Ndlwana, N. Raleie, K. M. Dimpe, H. F. Ogutu, E. O. Oseghe, M. M. Motsa, T. A. M. Msagati and B. B. Mamba, *Materials*, 2021, **14**, 5094.
99 S. R. Khapate, T. A. J. Siddiqui and R. S. Mane, in *Chapter 6 - Solvothermal Technique for the Synthesis of Metal Oxide Nanostructures*, ed. R. Mane, V. Jadhav and A. Al-Enizi, Elsevier, 2023, p. 95.
100 S. R. Khapate, T. A. Siddiqui and R. S. Mane, *Solvothermal Technique for the Synthesis of Metal Oxide Nanostructures*, Elsevier. 2023, p. 95.
101 L. Sun, G. Yuan, L. Gao, J. Yang, M. Chhowalla, M. H. Gharahcheshmeh, K. K. Gleason, Y. S. Choi, B. H. Hong and Z. Liu, *Nat. Rev. Methods Primers*, 2021, **1**, 5.
102 S. H. Li, M. Y. Qi, Z. R. Tang and Y. J. Xu, *Chem. Soc. Rev.*, 2021, **50**, 7539.
103 L. Tang, J. Tan, H. Nong, B. Liu and H.-M. Cheng, *Acc. Mater. Res.*, 2020, **2**, 36.
104 A. Tombesi, S. Li, S. Sathasivam, K. Page, F. L. Heale, C. Pettinari, C. J. Carmalt and I. P. Parkin, *Sci. Rep.*, 2019, **9**, 7549.
105 D. Vernardou, *Advances in Chemical Vapor Deposition*, MDPI, 2020, p. 4167.
106 M. Saeed, Y. Alshammari, S. A. Majeed and E. Al-Nasrallah, *Molecules*, 2020, **25**, 3856.
107 B. Qin, H. Ma, M. Hossain, M. Zhong, Q. Xia, B. Li and X. Duan, *Chem. Mater.*, 2020, **32**, 10321.
108 R. Kumar, N. Goel, D. K. Jarwal, Y. Hu, J. Zhang and M. Kumar, *J. Mater. Chem. C*, 2023, **11**, 774.
109 I. Sayago, E. Hontañón and M. Aleixandre, *Tin Oxide Materials*, 2020, p. 247.
110 F. Tu, M. Drost, S. Imre, J. Kiss, Z. Kónya and H. Marbach, *Beilstein J. Nanotechnol.*, 2017, **8**, 2592.
111 T. T. Nguyen, J. Balamurugan, N. H. Kim and J. H. Lee, *J. Mater. Chem. A*, 2018, **6**, 8669.
112 Z. Liu, S. Yang, B. Sun, X. Chang, J. Zheng and X. Li, *Angew. Chem., Int. Ed.*, 2018, **57**, 10187.
113 Y. Jiang, Y. Wang, J. Jiang, S. Liu, W. Li, S. Huang, Z. Chen and B. Zhao, *Electrochim. Acta*, 2019, **312**, 263.
114 D. Zhu, Q. Zhen, J. Xin, H. Ma, L. Tan, H. Pang and X. Wang, *Sens. Actuators, B*, 2020, **321**, 128541.
115 A. Agarwal and B. R. Sankapal, *J. Mater. Chem. A*, 2021, **9**, 20241.
116 J. Nai and X. W. Lou, *Adv. Mater.*, 2019, **31**, 1706825.
117 X. Li and J. Wang, *Adv. Mater. Interfaces*, 2020, **7**, 2000676.
118 F. Chen, J. Xu, S. Wang, Y. Lv, Y. Li, X. Chen, A. Xia, Y. Li, J. Wu and L. Ma, *Advanced Science*, 2022, **9**, 2200740.
119 X. Yi, Y. Guo, S. Chi, S. Pan, C. Geng, M. Li, Z. Li, W. Lv, S. Wu and Q. H. Yang, *Adv. Funct. Mater.*, 2023, **33**, 2303574.
120 X. F. Lu, S. L. Zhang, W. L. Sim, S. Gao and X. W. Lou, *Angew. Chem.*, 2021, **133**, 23067.
121 R. Schlem, C. F. Burmeister, P. Michalowski, S. Ohno, G. F. Dewald, A. Kwade and W. G. Zeier, *Adv. Energy Mater.*, 2021, **11**, 2101022.
122 M. Bianchini, J. Wang, R. J. Clément, B. Ouyang, P. Xiao, D. Kitchaev, T. Shi, Y. Zhang, Y. Wang and H. Kim, *Nat. Mater.*, 2020, **19**, 1088.
123 B. Wang, C. Zhang, W. Zheng, Q. Zhang, Z. Bao, L. Kong and L. Li, *Chem. Mater.*, 2019, **32**, 308.
124 X. Zhu, G. H. ten Brink, S. de Graaf, B. J. Kooi and G. Palasantzas, *Chem. Mater.*, 2020, **32**, 1627.
125 S. Gaan, *Evaluation of Gas Phase: Mechanisms and Analyses*, Elsevier., 2022, p. 117.
126 G. M. Tomboc, Y. Wang, H. Wang, J. Li and K. Lee, *Energy Storage Mater.*, 2021, **39**, 21.
127 W. Liu, H. Zhi and X. Yu, *Energy Storage Mater.*, 2019, **16**, 290.
128 L. Su, H. Li, Y. Xiao, G. Han and M. Zhu, *J. Alloys Compd.*, 2019, **771**, 117.
129 G. Chen, S. Tang, Y. Song, X. Meng, J. Yin, Y. Xia and Z. Liu, *Chem. Eng. J.*, 2019, **361**, 387.
130 N. Jiang, S. Shi, Y. Cui and B. Jiang, *J. Alloys Compd.*, 2022, **929**, 167229.
131 J. H. Bang and K. S. Suslick, *Adv. Mater.*, 2010, **22**, 1039.
132 S. V. Ley and C. M. Low, *Ultrasound in Synthesis*, Springer Science & Business Media, 2012.
133 A. Usman, A. Aris, B. Labaran, M. Darwish, A. Jagaba and J. New Mater, *Electrochem. Syst.*, 2022, **25**, 251.
134 X. Lv and L. Xiang, *Nanomaterials*, 2022, **12**, 3021.
135 N. Kumari, S. Kumar, P. Chauhan, G. A. Kaur, I. Kainthla and M. Shandilya, *J. Inorg. Organomet. Polym. Mater.*, 2024, 1.
136 C. R. Bandeira, A. R. Dória, J. Y. C. Ribeiro, L. R. Prado, R. A. de Jesus, H. M. C. Andrade, R. S. de Santana Castro, L. F. R. Ferreira, S. M. Egues and R. T. Figueiredo, *Mater. Chem. Phys.*, 2021, **265**, 124521.
137 N. A. Neto, A. Lima, R. Wilson, T. Nicacio, M. Bomio and F. Motta, *Mater. Sci. Semicond. Process.*, 2022, **139**, 106311.
138 P. Mohanty, R. Mahapatra, P. Padhi, C. V. Ramana and D. K. Mishra, *Nano-Struct. Nano-Objects*, 2020, **23**, 100475.
139 M. Amar, M. Benzerzour, J. Kleib and N.-E. Abriak, *Int. J. Sediment Res.*, 2020, **36**(1), 92–109.
140 B. Kalsi, S. Singh and M. Alam, *J. Food Process Eng.*, 2023, **46**(6), e14163.

141 R. Han, Y. Wang, S. Xing, C. Pang, Y. Hao, C. Song and Q. Liu, *Chem. Eng. J.*, 2022, **450**, 137952.
142 B. Purnama and A. T. Wijayanta, *J. King Saud Univ., Sci.*, 2019, **31**, 956.
143 G. Zhu, C. Zhang, C. Zhang and Y. Yi, *Chem. Eng. J.*, 2024, **497**, 154512.
144 A. K. Soni, R. Joshi and R. S. Ningthoujam, in *Hot Injection Method for Nanoparticle Synthesis: Basic Concepts, Examples and Applications*, ed. A. K. Tyagi and R. S. Ningthoujam, Springer Singapore, Singapore, 2021, p. 383.
145 J. Yuan, Y. Zhang, F. Chen and Z. Gu, *J. Mater. Chem. C*, 2024, 14729.
146 X. Li, W. Xing, T. Hu, K. Luo, J. Wang and W. Tang, *Coord. Chem. Rev.*, 2022, **473**, 214811.
147 F. Bu, W. Chen, M. F. Aly Aboud, I. Shakir, J. Gu and Y. Xu, *J. Mater. Chem. A*, 2019, **7**, 14526.
148 L. Yang, X. Yuan, W. Liang, R. Song, Q. Wang, C. Chen and Z. Bai, *Catal. Lett.*, 2024, 4116.
149 J. Zheng, M. S. Kim, Z. Tu, S. Choudhury, T. Tang and L. A. Archer, *Chem. Soc. Rev.*, 2020, **49**, 2701.
150 V. T. Chebrolu, B. Balakrishnan, S. Aravindha Raja, I. Cho, J.-S. Bak and H.-J. Kim, *New J. Chem.*, 2020, **44**, 7690.
151 H. Wu, X. Li, L. Chen and Y. Dan, *Batteries Supercaps*, 2019, **2**, 144.
152 A. Agarwal and T. Soga, in *Electroless Assisted Nanostructured Morphologies*, ed. B. R. Sankapal, A. Ennaoui, R. B. Gupta and C. D. Lokhande, Springer Nature Singapore, Singapore, 2023, p. 211.
153 A. Ramesh, S. Basu and M. Sterlin Leo Hudson, in *Polymer-Metal Phosphide Nanocomposites for Flexible Supercapacitors*, ed. R. K. Gupta, Springer Nature Singapore, Singapore, 2023, pp. 283.
154 H.-K. Kang and H.-C. Shin, *J. Electrochem. Sci. Technol.*, 2020, **11**, 155.
155 S. Battiato, L. Bruno, A. L. Pellegrino, A. Terrasi and S. Mirabella, *Catal. Today*, 2023, **423**, 113929.
156 G. Chen, R. Li and L. Huang, *Nanoscale*, 2023, **15**, 13909.
157 A. Kumar, P. Choudhary, A. Kumar, P. H. C. Camargo and V. Krishnan, *Small*, 2022, **18**, e2101638.
158 K. Li, X. Chen, J. Zhao, H. She, J. Huang, L. Wang and Q. Wang, *ACS Appl. Energy Mater.*, 2022, **5**, 10207.
159 M. Z. Iqbal, M. M. Faisal, M. Sulman, S. R. Ali, A. M. Afzal, M. A. Kamran and T. Alharbi, *J. Energy Storage*, 2020, **29**, 101324.
160 R. M. A. Hameed, Nanostructured Phosphides as Electrocatalysts for Green Energy Generation, *Am. Chem. Soc.*, 2022, 191.
161 F. Foroughi, J. J. Lamb, O. S. Burheim and B. G. Pollet, *Catalysts*, 2021, **11**, 284.
162 Z. Li, J. Yang, T. Guang, B. Fan, K. Zhu and X. Wang, *Small Methods*, 2021, **5**, 2100193.
163 W. Zhang, J. Bao, C. Lu, X. Zhou, X. Xia, J. Zhang, X. He, Y. Gan, H. Huang, C. Wang, W. Wan, R. Fang and Y. Xia, *J. Solid State Electrochem.*, 2023, 51.
164 H. Tan, L. Sun, Y. Zhang, K. Wang and Y. Zhang, *Adv. Sustainable Syst.*, 2022, **6**(9), 2200183.
165 Z. A. Zeenat, M. Maqbool, M. Asif Hussain, R. Adel Pashameah, A. Shahzadi, N. Nazar, S. Iqbal, A. K. Alanazi, M. Naeem Ashiq and H. M. Abo-Dief, *Fuel*, 2023, **331**, 125913.
166 Y. Yang, Y. Zhou, Z. Hu, W. Wang, X. Zhang, L. Qiang and Q. Wang, *J. Alloys Compd.*, 2019, **772**, 683.
167 Z. Jia, X. Kong, Z. Liu, X. Zhao, X. Zhao, F. He, Y. Zhao, M. Zhang and P. Yang, *ChemSusChem*, 2024, **17**, e202301386.
168 Y. Jeung, H. Jung, D. Kim, H. Roh, C. Lim, J. W. Han and K. Yong, *J. Mater. Chem. A*, 2021, **9**, 12203.
169 M. Malekzadeh and M. T. Swihart, *Chem. Soc. Rev.*, 2021, **50**, 7132.
170 F. W. Eagle, R. A. Rivera-Maldonado and B. M. Cossairt, *Annu. Rev. Mater. Res.*, 2021, **51**, 541.
171 G. E. Ayom, M. D. Khan, J. Choi, R. K. Gupta, W. E. van Zyl and N. Revaprasadu, *Dalton Trans.*, 2021, **50**, 11821.
172 A. K. Tyagi and R. S. Ningthoujam, In *Handbook on Synthesis Strategies for Advanced Materials*, Springer, 2021.
173 X. Tang, S. Gao, D. Zhang, X. Xia, J. Wang, W. She, B. Yang, X. Meng, K. Wang, Z. Han and B. Wang, *J. Alloys Compd.*, 2022, **923**, 166289.
174 C. Lin, L. Ouyang, R. Hu, J. Liu, L. Yang, H. Shao and M. Zhu, *Prog. Nat. Sci.:Mater. Int.*, 2021, **31**, 567.
175 S. Liu, C. Luo, L. Chai and J. Ren, *J. Solid State Electrochem.*, 2021, **25**, 1975.
176 X. Liu, Y. Guo, W. Zhan and T. Jin, *Catalysts*, 2019, **9**, 240.
177 C. A. Downes, K. M. Van Allsburg, S. A. Tacey, K. A. Unocic, F. G. Baddour, D. A. Ruddy, N. J. LiBretto, M. M. O'Connor, C. A. Farberow, J. A. Schaidle and S. E. Habas, *Chem. Mater.*, 2022, **34**, 6255.
178 S.-B. Guo, W.-B. Zhang, Z.-Q. Yang, X. Bao, L. Zhang, Y.-W. Guo, X.-W. Han and J. Long, *Crystals*, 2022, 12.
179 Z. Li, Y. Zheng, Q. Liu, Y. Wang, D. Wang, Z. Li, P. Zheng and Z. Liu, *J. Mater. Chem. A*, 2020, **8**, 19113.
180 S. Dou, J. Xu, X. Cui, W. Liu, Z. Zhang, Y. Deng, W. Hu and Y. Chen, *Adv. Energy Mater.*, 2020, **10**(33), 2001331.
181 H.-M. Zhang, J.-J. Wang, Y. Meng and J. Sun, *Int. J. Hydrogen Energy*, 2022, **47**, 36084.
182 P. Zhang, W. Wang, Z. Kou, J. Li, T. Wang and J. Guo, *Ionics*, 2021, **27**, 801.
183 X. Wu, S. Chen, Y. Feng, Q. Yuan, J. Gao, Y. Chen, Y. Huang, Y. B. He and W. Gan, *Mater. Today Phys.*, 2019, **9**, 100132.
184 J. Xu, A. Schulte, H. Schönherr, X. Jiang and N. Yang, *Small Struct.*, 2021, **3**(2), 2100183.
185 S. Rafai, C. Qiao, Z. Wang, C. Cao, T. Mahmood, M. Naveed, W. Younas and S. Khalid, *ChemElectroChem*, 2019, **6**, 5469.
186 S. Song, M. Guo, S. Zhang, K. Zhan, Y. Yan, J. Yang, B. Zhao and M. Xu, *Electrochim. Acta*, 2020, **331**, 135431.
187 G.-d. Yi, C.-l. Fan, Z. Hu, W.-h. Zhang, S.-c. Han and J.-s. Liu, *Electrochim. Acta*, 2021, **383**, 138370.
188 J. Xu, N. Yang, S. Yu, A. Schulte, H. Schonherr and X. Jiang, *Nanoscale*, 2020, **12**, 13618.
189 M. Wang, H. Xu, L. Zhou, T. Sun and Y. Tang, *New J. Chem.*, 2024, **48**, 1200.
190 Y. Li, X. Wang, J. Meng, M. Song, M. Jiao, Q. Qin and L. Mi, *New J. Chem.*, 2023, **47**, 15143.

191 L. Huang, Y. Yang, C. Zhang, H. Yu, T. Wang, X. Dong, D. Li and Z. Liu, *Nanotechnology*, 2020, **31**, 225403.
192 X. Wang, J. Dai, H. Xie, C. Yang, L. He, T. Wu, X. Liu, Y. Xu, C. Yuan and L. Dai, *Chem. Eng. J.*, 2022, **438**, 135544.
193 Z. Fu, Z. Jiang, T. Hu and Z.-J. Jiang, *Electrochim. Acta*, 2022, **419**, 140392.
194 J. Cai, X. Zhang, Y. Pan, Y. Kong and S. Lin, *Int. J. Hydrogen Energy*, 2021, **46**, 34252.
195 Z. L. Choong, B. T. Goh, M. L. Ooi, K. C. Lau, R. C. S. Wong and K. W. Tan, *Thin Solid Films*, 2024, **788**, 140150.
196 H.-b. Zheng, Y.-l. Li, Y.-l. Wang, F. Ma, P.-z. Gao, W.-m. Guo, H. Qin, X.-p. Liu and H.-n. Xiao, *J. Alloys Compd.*, 2022, **894**, 162411.
197 Q. Luo, L. Sun, Y. Zhao, C. Wang, H. Xin, D. Li and F. Ma, *J. Mater. Sci. Technol.*, 2023, **145**, 165.
198 M. Song, Y. Liu, J. Hong, X. Wang and X. Huang, *J. Adv. Ceram.*, 2023, **12**, 1872.
199 S. Duraisamy, A. Ganguly, P. K. Sharma, J. Benson, J. Davis and P. Papakonstantinou, *ACS Appl. Nano Mater.*, 2021, **4**, 2642.
200 S. Zhao, W. Xu, Z. Yang, X. Zhang and Q. Zhang, *Electrochim. Acta*, 2020, **331**, 135265.
201 B. Reddy, M. Premasudha, N. Reddy, H.-J. Ahn, J.-H. Ahn and K.-K. Cho, *J. Energy Storage*, 2021, **39**, 102660.
202 Y. Li, Y. Zhang, X. Tong, X. Wang, L. Zhang, X. Xia and J. Tu, *J. Mater. Chem. A*, 2021, **9**, 1418.
203 S. Liu, Y. Yin, M. Wu, K. S. Hui, K. N. Hui, C. Y. Ouyang and S. C. Jun, *Small*, 2019, **15**, 1803984.
204 F. Liu, N. Wang, C. Shi, J. Sha, L. Ma, E. Liu and N. Zhao, *Chem. Eng. J.*, 2022, **431**, 133923.
205 Y. T. Baheri, M. A. Hedayati, M. Maleki and H. Karimian, *J. Energy Storage*, 2023, **68**, 107682.
206 H. Cheng, R. Liu, R. Zhang, L. Huang and Q. Yuan, *Nanoscale Adv.*, 2023, **5**, 2394.
207 S. Sarwar, M.-C. Lin, M. R. Ahasan, Y. Wang, R. Wang and X. Zhang, *Adv. Compos. Hybrid Mater.*, 2022, **5**, 2339.
208 N. H. A. Rosli, K. S. Lau, T. Winie, S. X. Chin, S. Zakaria and C. H. Chia, *J. Energy Storage*, 2022, **52**, 104991.
209 Y. Wang, T. Ge, X. Zhan, S. Liu, Y. Wei and Y. Qiao, *J. Sulfur Chem.*, 2024, 1.
210 R. Levinas, N. Tsyntsaru and H. Cesiulis, *Electrochim. Acta*, 2019, **317**, 427.
211 A. Teli, S. Beknalkar, S. Mane, T. Bhat, B. Kamble, S. Patil, S. Sadale and J. Shin, *Ceram. Int.*, 2022, **48**, 29002.
212 J. Zhao, H. Ren, C. Gu, W. Guan, X. Song and J. Huang, *J. Alloys Compd.*, 2019, **781**, 174.
213 D. Saha, V. Patel, P. R. Selvaganapathy and P. Kruse, *Nanoscale Adv.*, 2022, **4**, 125.
214 Q. Zhang, W. He, Y. Wang, D. Pei and X. Zheng, *Nano*, 2019, **14**, 1950055.
215 Y. Liu and R. Li, *Ultrason. Sonochem.*, 2020, **63**, 104923.
216 H. Wang, L. Geng, Z. Zhang, P. Zhong, F. Liu, Y. Xie, Y. Zhao, P. Li and X. Ma, *Nanotechnology*, 2023, **34**, 375601.
217 L. N. Khandare, D. J. Late and N. B. Chaure, *J. Energy Storage*, 2023, **74**, 109336.
218 C. A. Beaudette, J. T. Held, K. A. Mkhoyan and U. R. Kortshagen, *ACS Omega*, 2020, **5**, 21853.
219 D. He, Y. Yang, Z. Liu, J. Shao, J. Wu, S. Wang, L. Shen and N. Bao, *Nano Res.*, 2020, **13**, 1029.
220 H. Ganesha, S. Veeresh, Y. Nagaraju, M. Vandana, M. Basappa, H. Vijeth and H. Devendrappa, *Nanoscale Adv.*, 2022, **4**, 521.
221 Q. Lin, X. Dong, Y. Wang, N. Zheng, Y. Zhao, W. Xu and T. Ding, *J. Mater. Sci.*, 2020, **55**, 6637.
222 V. Klimas, C. Bittencourt, G. Valušis and A. Jagminas, *Mater. Charact.*, 2021, **179**, 111351.
223 H. Liu, M. Zhang, Z. Song, T. Ma, Z. Huang, A. Wang and S. Shao, *J. Alloys Compd.*, 2021, **881**, 160660.
224 C. He, W. Yin, X. Li, J. Zheng, B. Tang and Y. Rui, *Electrochim. Acta*, 2021, **365**, 137353.
225 X. Wang, W. You, L. Yang, G. Chen, Z. Wu, C. Zhang, Q. Chen and R. Che, *Nanoscale Adv.*, 2022, **4**, 3398.
226 D. Chen, J. Xiao, H. Zhou and A. Yuan, *ChemistrySelect*, 2020, **5**, 3130.
227 G.-A. Li, C.-Y. Wang, W.-C. Chang and H.-Y. Tuan, *ACS Nano*, 2016, **10**, 8632.
228 J. Yu, Q. Li, Y. Li, C.-Y. Xu, L. Zhen, V. P. Dravid and J. Wu, *Adv. Funct. Mater.*, 2016, **26**, 7644.
229 F. Yang, N. Kang, J. Yan, X. Wang, J. He, S. Huo and L. Song, *Metals*, 2018, **8**, 359.
230 Q. Zhou, J. Feng, X. Peng, L. Zhong and R. Sun, *J. Energy Chem.*, 2020, **45**, 45.
231 M. H. Suliman, A. Adam, L. Li, Z. Tian, M. N. Siddiqui, Z. H. Yamani and M. Qamar, *ACS Sustain. Chem. Eng.*, 2019, **7**, 17671.
232 Y. Shi, M. Li, Y. Yu and B. Zhang, *Energy Environ. Sci.*, 2020, **13**, 4564.
233 S. Imani Yengejeh, J. Liu, S. A. Kazemi, W. Wen and Y. Wang, *ACS Omega*, 2020, **5**, 5994.
234 Y. Li, R. Li, D. Wang, H. Xu, F. Meng, D. Dong, J. Jiang, J. Zhang, M. An and P. Yang, *Int. J. Hydrogen Energy*, 2021, **46**, 5131.
235 N. Attarzadeh, D. Das, S. N. Chintalapalle, S. Tan, V. Shutthanandan and C. Ramana, *ACS Appl. Mater. Interfaces*, 2023, **15**, 22036.
236 Z. Zhu, Y. Tang, W. R. Leow, H. Xia, Z. Lv, J. Wei, X. Ge, S. Cao, Y. Zhang and W. Zhang, *Angew. Chem.*, 2019, **131**, 3559.
237 T. Chen, H. Zou, X. Wu, C. Liu, B. Situ, L. Zheng and G. Yang, *ACS Appl. Mater. Interfaces*, 2018, **10**, 12453.
238 X. Hu, P. Jiang, J. Wan, Y. Xu and X. Sun, *J. Coat. Technol. Res.*, 2009, **6**, 275.
239 X. Feng and H. Yang, *J. Vinyl Addit. Technol.*, 2023, **29**, 522.
240 H. Chen, X. Liang, Y. Liu, X. Ai, T. Asefa and X. Zou, *Adv. Mater.*, 2020, **32**, 2002435.
241 A. Altuntepe, S. Erkan, M. A. Olğar, S. Çelik and R. Zan, *Int. J. Hydrogen Energy*, 2024, **56**, 690.
242 J. Park, S. Bhoyate, Y.-H. Kim, Y.-M. Kim, Y. H. Lee, P. Conlin, K. Cho and W. Choi, *ACS Nano*, 2021, **15**, 12267.
243 D. Sahoo, J. Shakya, N. Ali, W. J. Yoo and B. Kaviraj, *Langmuir*, 2022, **38**, 1578.
244 G. Swain, S. Sultana and K. Parida, *Nanoscale*, 2021, **13**, 9908.

245 G. Liu, L. Ding, Y. Meng, A. Ali, G. Zuo, X. Meng, K. Chang, O. L. Li and J. Ye, *Carbon Energy*, 2024, **6**, e521.
246 L. Zhao, Y. Li, M. Yu, Y. Peng and F. Ran, *Advanced Science*, 2023, **10**, 2300283.
247 X. Qin, B. Yan, D. Kim, Z. Teng, T. Chen, J. Choi, L. Xu and Y. Piao, *Appl. Catal., B*, 2022, **304**, 120923.
248 Q. Wang, F. Jia, S. Song and Y. Li, *Sep. Purif. Technol.*, 2020, **236**, 116298.
249 Y. Yao, J. He, X. Zhu, L. Mu, J. Li, K. Li and M. Qu, *Int. J. Hydrogen Energy*, 2024, **51**, 207.
250 S. Das, G. Swain and K. Parida, *Mater. Chem. Front.*, 2021, **5**, 2143.
251 R. Mohili, N. Hemanth, H. Jin, K. Lee and N. Chaudhari, *J. Mater. Chem. A*, 2023, **11**, 10463.
252 F. Fioravanti, S. Martínez, S. Delgado, G. García, J. L. Rodriguez, E. P. Tejera and G. I. Lacconi, *Electrochim. Acta*, 2023, **441**, 141781.
253 X. Li, X. Wang, Z. Sun, F. Li, Y. Fu, K. Zhao, G. Zhao, C. Zhu and X. Xu, *Chem. Eng. J.*, 2024, **495**, 153381.
254 P. Wang, X. Wang, R. Diao, Y. Guo, Y. Wang, C. Zhou, K.-F. Xie, S. Sun and Y.-H. Zhang, *J. Mater. Sci.: Mater. Electron.*, 2021, **32**, 14047.
255 S. Zhao, J. Xu, Z. Li, Z. Liu and Y. Li, *J. Colloid Interface Sci.*, 2019, **555**, 689.
256 V.-D. Hodoroaba, *Energy-dispersive X-Ray Spectroscopy (EDS)*, Elsevier, 2020, p. 397.
257 L. E. Franken, K. Grünewald, E. J. Boekema and M. C. Stuart, *Small*, 2020, **16**, 1906198.
258 S. E. Jun, S. Choi, S. Choi, T. H. Lee, C. Kim, J. W. Yang, W.-O. Choe, I.-H. Im, C.-J. Kim and H. W. Jang, *Nano-Micro Lett.*, 2021, **13**, 81.
259 S. A. Chambers, *Surf. Sci. Rep.*, 2024, **79**, 100638.
260 T. Wang, J. Liu, Y. Ma, S. Han, C. Gu and J. Lian, *Electrochim. Acta*, 2021, **392**, 138976.
261 C. Lu, W. An, T. Shen, T. Cao, Y. Gao, K. Wang, Y. Wong, C. Cao, C. Wang, G. Huang and S. Xu, *Int. J. Hydrogen Energy*, 2024, **77**, 203.
262 C. Dang, P. Feng, S. He, L. Zhao, A. Shan, M. Li, L. Kong and L. Gao, *Electrochim. Acta*, 2023, **462**, 142771.
263 L. Wan, Y. Wang, Y. Zhang, C. Du, J. Chen, M. Xie, Z. Tian and W. Zhang, *J. Power Sources*, 2021, **506**, 230096.
264 X. Pu, D. Zhao, C. Fu, Z. Chen, S. Cao, C. Wang and Y. Cao, *Angew. Chem., Int. Ed.*, 2021, **60**, 21310.
265 T. Kim, W. Choi, H.-C. Shin, J.-Y. Choi, J. M. Kim, M.-S. Park and W.-S. Yoon, *J. Electrochem. Sci. Technol.*, 2020, **11**, 14.
266 A. Patra, K. Namsheer, J. R. Jose, S. Sahoo, B. Chakraborty and C. S. Rout, *J. Mater. Chem. A*, 2021, **9**, 25852.
267 S. Aderyani, P. Flouda, S. Shah, M. Green, J. Lutkenhaus and H. Ardebili, *Electrochim. Acta*, 2021, **390**, 138822.
268 L. Wang, M. Huang, J. Huang, X. Tang, L. Li, M. Peng, K. Zhang, T. Hu, K. Yuan and Y. Chen, *J. Mater. Chem. A*, 2021, **9**, 15404.
269 Q. Zong, C. Liu, H. Yang, Q. Zhang and G. Cao, *Nano Today*, 2021, **38**, 101201.
270 J. Zhang, H. Yu, J. Yang, X. Zhu, M. Hu and J. Yang, *J. Alloys Compd.*, 2022, **924**, 166613.
271 O. Gharbi, M. T. Tran, B. Tribollet, M. Turmine and V. Vivier, *Electrochim. Acta*, 2020, **343**, 136109.
272 A. G. Kenesi, M. Ghorbani and M. S. Lashkenari, *Int. J. Hydrogen Energy*, 2022, **47**, 38849.
273 B. Ramulu, J. A. Shaik, A. R. Mule and J. S. Yu, *Mater. Sci. Eng., R*, 2024, **160**, 100820.
274 H. Rashid Khan and A. Latif Ahmad, *J. Ind. Eng. Chem.*, 2025, **141**, 46.
275 Y. Jin, H. Ao, K. Qi, X. Zhang, M. Liu, T. Zhou, S. Wang, G. Xia and Y. Zhu, *Mater. Today Energy*, 2021, **19**, 100598.
276 W. Zhao, L. Zou, L. Zhang, X. Fan, H. Zhang, F. Pagani, E. Brack, L. Seidl, X. Ou and K. Egorov, *Small*, 2022, **18**, 2107357.
277 N. O. Laschuk, E. B. Easton and O. V. Zenkina, *RSC Adv.*, 2021, **11**, 27925.
278 V. Vivier and M. E. Orazem, *Chem. Rev.*, 2022, **122**, 11131.
279 H. S. Magar, R. Y. Hassan and A. Mulchandani, *Sensors*, 2021, **21**, 6578.
280 A. C. Lazanas and M. I. Prodromidis, *ACS Meas. Sci. Au*, 2023, **3**, 162.
281 L. A. Santa-Cruz, F. C. Tavares, L. F. Loguercio, C. I. Dos Santos, R. A. Galvão, O. A. Alves, M. Z. Oliveira, R. M. Torresi and G. Machado, *Phys. Chem. Chem. Phys.*, 2024, **26**(40), 25748–25761.
282 M. Y. Perdana, B. A. Johan, M. Abdallah, M. E. Hossain, M. A. Aziz, T. N. Baroud and Q. A. Drmosh, *Chem. Rec.*, 2024, **24**, e202400007.
283 A. Kalair, N. Abas, M. S. Saleem, A. R. Kalair and N. Khan, *Energy Storage*, 2021, **3**, e135.
284 A. G. Olabi, Q. Abbas, A. Al Makky and M. A. Abdelkareem, *Energy*, 2022, **248**, 123617.
285 G. Z. Chen, *Int. Mater. Rev.*, 2017, **62**, 173.
286 J. Li, T. Xiao, X. Yu and M. Wang, *J. Phys.: Conf. Ser.*, 2022, **2393**, 012005.
287 J. Wu, *Chem. Rev.*, 2022, **122**, 10821.
288 N. Swain, B. Saravanakumar, M. Kundu, L. Schmidt-Mende and A. Ramadoss, *J. Mater. Chem. A*, 2021, **9**, 25286.
289 P. Bhojane, *J. Energy Storage*, 2022, **45**, 103654.
290 D. P. Chatterjee and A. K. Nandi, *J. Mater. Chem. A*, 2021, **9**, 15880.
291 T. Schoetz, L. Gordon, S. Ivanov, A. Bund, D. Mandler and R. Messinger, *Electrochim. Acta*, 2022, **412**, 140072.
292 A. Hu, F. Li, W. Chen, T. Lei, Y. Li, Y. Fan, M. He, F. Wang, M. Zhou and Y. Hu, *Adv. Energy Mater.*, 2022, **12**, 2202432.
293 O. C. Esan, X. Shi, Z. Pan, X. Huo, L. An and T. Zhao, *Adv. Energy Mater.*, 2020, **10**, 2000758.
294 C. Li, B. Liu, N. Jiang and Y. Ding, *Nano Res. Energy*, 2022, **1**(3), 9120031.
295 M. Weiss, R. Ruess, J. Kasnatscheew, Y. Levartovsky, N. R. Levy, P. Minnmann, L. Stolz, T. Waldmann, M. Wohlfahrt-Mehrens and D. Aurbach, *Adv. Energy Mater.*, 2021, **11**, 2101126.
296 G. Wang, M. Yu and X. Feng, *Chem. Soc. Rev.*, 2021, **50**, 2388.
297 P. Shi, L.-P. Hou, C.-B. Jin, Y. Xiao, Y.-X. Yao, J. Xie, B.-Q. Li, X.-Q. Zhang and Q. Zhang, *J. Am. Chem. Soc.*, 2021, **144**, 212.

298 W. H. Li, Q. L. Ning, X. T. Xi, B. H. Hou, J. Z. Guo, Y. Yang, B. Chen and X. L. Wu, *Adv. Mater.*, 2019, **31**, 1804766.
299 Y. Lv, M. Zhao, Y. Du, Y. Kang, Y. Xiao and S. Chen, *Energy Environ. Sci.*, 2022, **15**, 4748.
300 R. Yuan, Y. Dong, R. Hou, S. Zhang and H. Song, *J. Electrochem. Soc.*, 2022, **169**, 030504.
301 A. Roy, M. Sotoudeh, S. Dinda, Y. Tang, C. Kübel, A. Groß, Z. Zhao-Karger, M. Fichtner and Z. Li, *Nat. Commun.*, 2024, **15**, 492.
302 H. Wu, C. Feng, L. Zhang, J. Zhang and D. P. Wilkinson, *Electrochem. Energy Rev.*, 2021, **4**, 473.
303 P. Moriarty and D. Honnery, *Int. J. Hydrogen Energy*, 2019, **44**, 16029.
304 S. E. Hosseini and M. A. Wahid, *Int. J. Energy Res.*, 2020, **44**, 4110.
305 N. Mahmood, Y. Yao, J. W. Zhang, L. Pan, X. Zhang and J. J. Zou, *Advanced Science*, 2018, **5**, 1700464.
306 N. Danilovic, R. Subbaraman, D. Strmcnik, V. Stamenkovic and N. Markovic, *J. Serb. Chem. Soc.*, 2013, **78**, 2007.
307 S. K. T. Aziz, S. Sultana, A. Kumar, S. Riyajuddin, M. Pal and A. Dutta, *Cell Rep. Phys. Sci.*, 2023, **4**, 101747.
308 Q. Yan, X. Chen, T. Wei, G. Wang, M. Zhu, Y. Zhuo, K. Cheng, K. Ye, K. Zhu and J. Yan, *ACS Sustain. Chem. Eng.*, 2019, **7**, 7804.
309 J. F. Callejas, J. M. McEnaney, C. G. Read, J. C. Crompton, A. J. Biacchi, E. J. Popczun, T. R. Gordon, N. S. Lewis and R. E. Schaak, *ACS Nano*, 2014, **8**, 11101.
310 T. Reier, H. N. Nong, D. Teschner, R. Schlögl and P. Strasser, *Adv. Energy Mater.*, 2017, **7**, 1601275.
311 X. Xie, L. Du, L. Yan, S. Park, Y. Qiu, J. Sokolowski, W. Wang and Y. Shao, *Adv. Funct. Mater.*, 2022, **32**, 2110036.
312 X. Hu, R. Wang, W. Feng, C. Xu and Z. Wei, *J. Energy Chem.*, 2023, **81**, 167.
313 C. Niu, G. Han, H. Song, S. Yuan and W. Hou, *J. Colloid Interface Sci.*, 2020, **561**, 117.
314 G. Li, Y. Feng, Y. Yang, X. Wu, X. Song and L. Tan, *Nano Mater. Sci.*, 2024, **6**, 174.
315 S. T. Aziz, S. Kumar, S. Riyajuddin, K. Ghosh, G. D. Nessim and D. P. Dubal, *J. Phys. Chem. Lett.*, 2021, **12**, 5138.
316 K. Prakash, S. Harish, K. Silambarasan, T. Logu, R. Ramesh, J. Archana and M. Navaneethan, *J. Colloid Interface Sci.*, 2022, **628**, 131.
317 Z. Zhao, Y. Duan, F. Chen, Z. Tian, R. Pathak, J. W. Elam, Z. Yi, Y. Wang and X. Wang, *Chem. Eng. J.*, 2022, **450**, 138310.
318 L. Liu, X. Yin, W. Li, D. Wang, J. Duan, X. Wang, Y. Zhang, D. Peng and Y. Zhang, *Small*, 2024, **20**, 2308564.
319 X. Qian, G. Zhu, K. Wang, F. Zhang, K. Liang, W. Luo and J. Yang, *Chem. Eng. J.*, 2020, **381**, 122651.
320 X. Zhang, M. Jia, Q. Zhang, N. Zhang, X. Wu, S. Qi and L. Zhang, *Chem. Eng. J.*, 2022, **448**, 137743.
321 G. Chang, Y. Zhao, L. Dong, D. P. Wilkinson, L. Zhang, Q. Shao, W. Yan, X. A. Sun and J. Zhang, *J. Mater. Chem. A*, 2020, **8**, 4996.
322 W. Hu, L. Xie, C. Gu, W. Zheng, Y. Tu, H. Yu, B. Huang and L. Wang, *Coord. Chem. Rev.*, 2024, **506**, 215715.
323 J. Bao, Y. Zhou, Y. Zhang, X. Sheng, Y. Wang, S. Liang, C. Guo, W. Yang, T. Zhuang and Y. Hu, *J. Mater. Chem. A*, 2020, **8**, 22181.
324 L. Li, Z. Qin, L. Ries, S. Hong, T. Michel, J. Yang, C. Salameh, M. Bechelany, P. Miele and D. Kaplan, *ACS Nano*, 2019, **13**, 6824.
325 Y. Hu, H. Yu, L. Qi, J. Dong, P. Yan, T. Taylor Isimjan and X. Yang, *ChemSusChem*, 2021, **14**, 1565.
326 H. K. Kim, H. Jang, X. Jin, M. G. Kim and S.-J. Hwang, *Appl. Catal., B*, 2022, **312**, 121391.
327 Y. Li, J. Meng, X. Wang, M. Song, M. Jiao, Q. Qin and L. Mi, *Dalton Trans.*, 2023, **52**, 14613.
328 S. Wang, G. Li, G. Du, X. Jiang, C. Feng, Z. Guo and S.-J. Kim, *Chin. J. Chem. Eng.*, 2010, **18**, 910.
329 H. Zhou, Y. Zhao, Y. Jin, Q. Fan, Y. Dong and Q. Kuang, *J. Power Sources*, 2023, **560**, 232715.
330 Z. Kong, Z. Liang, M. Huang, H. Tu, K. Zhang, Y. Shao, Y. Wu and X. Hao, *J. Alloys Compd.*, 2023, **930**, 167328.
331 Y. Xia, T. Yang, Z. Wang, T. Mao, Z. Hong, J. Han, D.-L. Peng and G. Yue, *Adv. Funct. Mater.*, 2023, **33**, 2302830.
332 M. Song, Y. Liu, J. Hong, X. Wang, X. Huang and J. Adv, *Ceram*, 2023, **12**, 1872.
333 Z. Xu, C. Du, H. Yang, J. Huang, X. Zhang and J. Chen, *Chem. Eng. J.*, 2021, **421**, 127871.
334 J. Wu, F. Yan, Z. Huang, J. Liu, H. Huang, Y. Liang, J. Li, F. Yuan, X. Liang, W. Zhou and J. Guo, *J. Energy Storage*, 2024, **97**, 112958.
335 H. Tan, Y. Zhang, Y. Geng, H. Li, S. Bi, Z. Xia, Q. Yang, Q. Wei and S. Chen, *Inorg. Chem.*, 2024, **63**, 13484.
336 J. Du, Q. Han, C. Liu, H. Wu, L. zheng and Z. Yang, *Appl. Surf. Sci.*, 2024, **649**, 159098.
337 Y. Jiang, S. Lei and M. Wang, *ACS Appl. Mater. Interfaces*, 2024, **16**, 30521.
338 W. Chen, X. Yan, Z. Liu, X. Zhang and C. Du, *Int. J. Hydrogen Energy*, 2023, **48**, 29969.
339 B. Zhang, K. Xu, X. Fu, S. Guan, X. Li and Z. Peng, *J. Alloys Compd.*, 2021, **856**, 158094.
340 A. Wu, Y. Gu, Y. Xie, C. Tian, H. Yan, D. Wang, X. Zhang, Z. Cai and H. Fu, *ACS Appl. Mater. Interfaces*, 2019, **11**, 25986.
341 Y. Jiang, Y. Lu, J. Lin, X. Wang and Z. Shen, *Small Methods*, 2018, **2**(5), 1700369.
342 D. Chen, J. Xiao, H. Zhou and A. Yuan, *ChemistrySelect*, 2020, **5**, 3130.
343 Z. Duan, H. Liu, X. Tan, A. Umar and X. Wu, *Catal. Commun.*, 2022, **162**, 106379.
344 Y.-R. Liu, W.-H. Hu, X. Li, B. Dong, X. Shang, G.-Q. Han, Y.-M. Chai, Y.-Q. Liu and C.-G. Liu, *Appl. Surf. Sci.*, 2016, **383**, 276.
345 D. Ma, K. Meng, J. Ma, Z. Jia, Y. Wang, L. Liu, G. Zhu and T. Qi, *Int. J. Hydrogen Energy*, 2019, **44**, 31960.
346 X. Zeng, H. Zhang, R. Yu, G. D. Stucky and J. Qiu, *J. Mater. Chem. A*, 2023, **11**, 14272.
347 A. Muthurasu, V. Maruthapandian and H. Y. Kim, *Appl. Catal., B*, 2019, **248**, 202.
348 M. Luo, S. Liu, W. Zhu, G. Ye, J. Wang and Z. He, *Chem. Eng. J.*, 2022, **428**, 131055.

349 Q. Wang, Z.-Y. Tian, W.-J. Cui, N. Hu, S.-M. Zhang, Y.-Y. Ma and Z.-G. Han, *Int. J. Hydrogen Energy*, 2022, **47**, 12629.
350 J. Xu, J. Rong, Y. Zheng, Y. Zhu, K. Mao, Z. Jing, T. Zhang, D. Yang and F. Qiu, *Electrochim. Acta*, 2021, **385**, 138438.
351 Y. Huang, X. Xie, Y. Zhang, J. Ding, L. Liu, Y. Fan, H. Lv, Y. Liu and Q. Cai, *Appl. Surf. Sci.*, 2020, **520**, 146340.
352 Z. Huang, X. Li, X. Xiang, T. Gao, Y. Zhang and D. Xiao, *J. Mater. Chem. A*, 2018, **6**, 23746.
353 Y. Hu, M. Liu, Q. Yang, L. Kong and L. Kang, *J. Energy Chem.*, 2017, **26**, 49.
354 B. Liang, Z. Zheng, M. Retana, K. Lu, T. Wood, Y. Ai, X. Zu and W. Zhou, *Nanotechnology*, 2019, **30**, 295401.
355 Y.-C. Chen, Z.-B. Chen, Y.-G. Lin and Y.-K. Hsu, *ACS Sustain. Chem. Eng.*, 2017, **5**, 3863.
356 J. Tian, H. Zhang and Z. Li, *ACS Appl. Mater. Interfaces*, 2018, **10**, 29511.
357 B. Wang, R. Hu, J. Zhang, Z. Huang, H. Qiao, L. Gong and X. Qi, *J. Am. Ceram. Soc.*, 2019, **103**, 1088.
358 A. Lathe, A. Ansari, R. Badhe, A. M. Palve and S. S. Garje, *ACS Omega*, 2021, **6**, 13008.
359 M. Manuraj, J. Chacko, K. N. Narayanan Unni and R. B. Rakhi, *J. Alloys Compd.*, 2020, **836**, 155420.
360 G. P. Awasthi, M. B. Poudel, M. Shin, K. P. Sharma, H. J. Kim and C. Yu, *J. Energy Storage*, 2021, **42**, 103140.
361 N. Chaudhary, A. Kumar, S. Imtiyaz and M. Khanuja, *ECS J. Solid State Sci. Technol.*, 2021, **10**, 053005.
362 D. Sahoo, J. Shakya, S. Choudhury, S. S. Roy, L. Devi, B. Singh, S. Ghosh and B. Kaviraj, *ACS Omega*, 2022, **7**, 16895.
363 F. Lu, J. Wang, X. Sun and Z. Chang, *Mater. Des.*, 2020, **189**, 108503.
364 A. Raza, A. Rasheed, A. Farid, M. Yousaf, N. Ayub and I. A. Khan, *J. Energy Storage*, 2024, **84**, 110811.
365 N. Chaudhary and M. Khanuja, *Energy Fuels*, 2021, **36**, 1034.
366 M. Yao, A. Liu, C. Xing, B. Li, S. Pan, J. Zhang, P. Su and H. Zhang, *Chem. Eng. J.*, 2020, **394**, 124883.
367 P. S. Shukla, A. Agrawal, A. Gaur and G. D. Varma, *J. Energy Storage*, 2023, **59**, 106580.
368 X. Liu, W. Yang, Z. Liu, H. Fan and W. Zheng, *Acta Metall. Sin.*, 2021, **34**, 401.
369 Z. Hu, L. Wang, K. Zhang, J. Wang, F. Cheng, Z. Tao and J. Chen, *Angew Chem. Int. Ed. Engl.*, 2014, **53**, 12794.
370 Y. Xia, T. Yang, Z. Wang, T. Mao, Z. Hong, J. Han, D. L. Peng and G. Yue, *Adv. Funct. Mater.*, 2024, **34**(6), 2310995.
371 Y. Yang, J. Xia, X. Guan, Z. Wei, J. Yu, S. Zhang, Y. Xing and P. Yang, *Small*, 2022, **18**, e2204970.
372 J. Liu, T. Zhou, T. Han, L. Zhu, Y. Wang, Y. Hu and Z. Chen, *Chem. Commun.*, 2022, **58**, 5108.
373 Y. Wang, L. Zhang, H. Li, Y. Wang, L. Jiao, H. Yuan, L. Chen, H. Tang and X. Yang, *J. Power Sources*, 2014, **253**, 360.
374 Y. Li, X. Yan, Z. Zhou, J. Liu, Z. Zhang, X. Guo, H. Peng and G. Li, *Appl. Surf. Sci.*, 2022, **574**, 151586.
375 D. Lei, W. Shang, X. Zhang, Y. Li, S. Qiao, Y. Zhong, X. Deng, X. Shi, Q. Zhang, C. Hao, X. Song and F. Zhang, *ACS Nano*, 2021, **15**, 20478.
376 Y. Zhao, M. Bi, F. Qian, P. Zeng, M. Chen, R. Wang, Y. Liu, Y. Ding and Z. Fang, *ChemElectroChem*, 2018, **5**, 3953.
377 B. Liu, D. Kong, Y. Wang, Y. V. Lim, S. Huang and H. Y. Yang, *FlatChem*, 2018, **10**, 14.
378 F. Chen, D. Shi, M. Yang, H. Jiang, Y. Shao, S. Wang, B. Zhang, J. Shen, Y. Wu and X. Hao, *Adv. Funct. Mater.*, 2020, **31**, 2009973.
379 Z. Wang, C. Cui, Y. Zhao, Q. Cui, H. Li, Z. Zhao, C. Wu and J. Wei, *J. Alloys Compd.*, 2023, **967**, 171820.
380 J. Zhang, W. Xi, F. Yu, Y. Zhang, R. Wang, Y. Gong, B. He, H. Wang and J. Jin, *Chem. Eng. J.*, 2023, **475**, 146009.
381 Z. Zhang, J. Zhao, M. Xu, H. Wang, Y. Gong and J. Xu, *Nanotechnology*, 2018, **29**, 335401.
382 L. Ma, X. Zhou, J. Sun, P. Zhang, B. Hou, S. Zhang, N. Shang, J. Song, H. Ye, H. Shao, Y. Tang and X. Zhao, *J. Energy Chem.*, 2023, **82**, 268.
383 J. Huang, Y. Yao, M. Huang, Y. Zhang, Y. Xie, M. Li, L. Yang, X. Wei and Z. Li, *Small*, 2022, **18**, e2200782.
384 T. Gu, J. Ren, S. Zhang, H. Guo, H. Wang, R.-P. Ren and Y.-K. Lv, *J. Alloys Compd.*, 2022, **901**, 163650.
385 B. Zhao, G. Suo, R. Mu, C. Lin, J. Li, X. Hou, X. Ye, Y. Yang and L. Zhang, *J. Colloid Interface Sci.*, 2024, **668**, 565.
386 T. Zhang, Y. Feng, J. Zhang, C. He, D. M. Itkis and J. Song, *Mater. Today Nano*, 2020, **12**, 100089.
387 L. Zhang, A. Xu, X. Shi, H. Zhang, Z. Wang, S. Shen, J. Zhang and W. Zhong, *RSC Adv.*, 2024, **14**, 19294.
388 M. Wang, H. Xu, L. Zhou, T. Sun and Y. Tang, *New J. Chem.*, 2024, **48**, 1200.
389 A. Wu, Y. Gu, Y. Xie, C. Tian, H. Yan, D. Wang, X. Zhang, Z. Cai and H. Fu, *ACS Appl. Mater. Interfaces*, 2019, **11**, 25986.
390 L. Zhang, A. Xu, X. Shi, H. Zhang, Z. Wang, S. Shen, J. Zhang and W. Zhong, *RSC Adv.*, 2024, **14**, 19294.
391 D. Meng, S. Ran, L. Gao, Y. Zhang, X. San, L. Zhang, R. Li and Q. Jin, *Chem. Res. Chin. Univ.*, 2024, **40**, 490.
392 Q. Luo, Y. Lv, P. Zhang, Z. Zhao, X. Bao, L. Guo, H. Luo, X. Fan, F. Ma, P-Mos2 Heterojunction as Self-Supported Electrode Enables Boosted Alkaline Hydrogen Evolution Reaction.
393 K. N. Dinh, Q. Liang, C.-F. Du, J. Zhao, A. I. Y. Tok, H. Mao and Q. Yan, *Nano Today*, 2019, **25**, 99.
394 X. Li, A. M. Elshahawy, C. Guan and J. Wang, *Small*, 2017, **13**, 1701530.
395 S. Bhat, J. Banday and M. Wahid, *Energy Fuels*, 2023, **37**, 6012.
396 Y. Cao, Z. Chen, F. Ye, Y. Yang, K. Wang, Z. Wang, L. Yin and C. Xu, *J. Alloys Compd.*, 2022, **896**, 163103.
397 X. Wang, G. Zhang, B. Wang, Y. Wu and S. Guo, *ACS Sustain. Chem. Eng.*, 2024, **12**, 14018.
398 Z. Zhao, D. E. Schipper, A. P. Leitner, H. Thirumalai, J.-H. Chen, L. Xie, F. Qin, M. K. Alam, L. C. Grabow and S. Chen, *Nano Energy*, 2017, **39**, 444.
399 K. Chen, L. Shi, Y. Zhang and Z. Liu, *Chem. Soc. Rev.*, 2018, **47**, 3018.
400 S. H. Choi, S. J. Yun, Y. S. Won, C. S. Oh, S. M. Kim, K. K. Kim and Y. H. Lee, *Nat. Commun.*, 2022, **13**, 1484.

401 Y. Zhang, K. Nie, L. Yi, B. Li, Y. Yuan, Z. Liu and W. Huang, *Advanced Science*, 2023, **10**, 2302301.
402 C. Ke, R. Shao, Y. Zhang, Z. Sun, S. Qi, H. Zhang, M. Li, Z. Chen, Y. Wang and B. Sa, *Adv. Funct. Mater.*, 2022, **32**, 2205635.
403 Y.-Y. Hsieh and H.-Y. Tuan, *Energy Storage Mater.*, 2022, **51**, 789.
404 T. Li, X. Hu, C. Yang, L. Han and K. Tao, *Dalton Trans.*, 2023, **52**, 16640.
405 C.-A. Chen, C.-L. Lee, P.-K. Yang, D.-S. Tsai and C.-P. Lee, *Catalysts*, 2021, **11**, 151.
406 Y.-h. Luo, Q.-l. Pan, H.-x. Wei, Y.-d. Huang, L.-b. Tang, Z.-y. Wang, C. Yan, J. Mao, K.-h. Dai and Q. Wu, *Mater. Today*, 2023, **69**, 54.
407 D. K. Bhat, H. Bantawal and U. S. Shenoy, *Diamond Relat. Mater.*, 2023, **139**, 110312.
408 H. Bai, D. Chen, Q. Ma, R. Qin, H. Xu, Y. Zhao, J. Chen and S. Mu, *Electrochem. Energy Rev.*, 2022, **5**, 24.
409 L. Yue, J. Liang, Z. Wu, B. Zhong, Y. Luo, Q. Liu, T. Li, Q. Kong, Y. Liu and A. M. Asiri, *J. Mater. Chem. A*, 2021, **9**, 11879.
410 H. Sun, X. Chu, Y. Zhu, B. Wang, G. Wang and J. Bai, *J. Electroanal. Chem.*, 2023, **932**, 117219.
411 X. Xu, Y. Pan, L. Ge, Y. Chen, X. Mao, D. Guan, M. Li, Y. Zhong, Z. Hu and V. K. Peterson, *Small*, 2021, **17**, 2101573.
412 S. Sanati, R. Abazari, J. Albero, A. Morsali, H. García, Z. Liang and R. Zou, *Angew. Chem., Int. Ed.*, 2021, **60**, 11048.
413 J. Li, Z. Xiong, Y. Wu, H. Li, X. Liu, H. Peng, Y. Zheng, Q. Zhang and Q. Liu, *J. Energy Chem.*, 2022, **73**, 513.
414 H. Yan, X. Xiao, C. Hu, X. Liu and Y. Song, *Mol. Catal.*, 2023, **547**, 113327.
415 P. Forouzandeh and S. C. Pillai, *Mater. Today: Proc.*, 2021, **41**, 498.
416 X. Wang, H.-M. Kim, Y. Xiao and Y.-K. Sun, *J. Mater. Chem. A*, 2016, **4**, 14915.
417 Z.-Z. Liu, N. Yu, R.-Y. Fan, B. Dong and Z.-F. Yan, *Nanoscale*, 2024, **16**, 1080.
418 J. Luo, Y. Wang, Y. Mao, Y. Zhang, Y. Su, B. Zou, S. Chen, Q. Deng, Z. Zeng and J. Wang, *Chem. Eng. J.*, 2022, **433**, 133549.
419 J. Yu, X. Wu, Y. Zhong, G. Yang, M. Ni, W. Zhou and Z. Shao, *Chem.–Eur. J.*, 2018, **24**, 13800.
420 Y. Xu, R. Wang, Z. Liu, L. Gao, T. Jiao and Z. Liu, *Green Energy Environ.*, 2022, **7**, 829.
421 Z. Li, X. Dou, Y. Zhao and C. Wu, *Inorg. Chem. Front.*, 2016, **3**, 1021.
422 J.-T. Ren, L. Chen, L. Wang, X.-L. Song, Q.-H. Kong and Z.-Y. Yuan, *J. Mater. Chem. A*, 2023, **11**, 2899.
423 R. Mohili, N. Hemanth, K. Lee and N. K. Chaudhari, *MXene-Transition Metal Compound Sulfide and Phosphide Hetero-Nanostructures for Photoelectrochemical Water Splitting*, Elsevier. 2023, pp. 129.
424 X. Chen, W. He, L.-X. Ding, S. Wang and H. Wang, *Energy Environ. Sci.*, 2019, **12**, 938.
425 S. Zhang, Y. Si, B. Li, L. Yang, W. Dai and S. Luo, *Small*, 2021, **17**, 2004980.
426 W. Li, Q. Song, M. Li, Y. Yuan, J. Zhang, N. Wang, Z. Yang, J. Huang, J. Lu and X. Li, *Small Methods*, 2021, **5**, 2100444.
427 M. Iqbal, E. Elahi, A. Amin, G. Hussain and S. Aftab, *Superlattices Microstruct.*, 2020, **137**, 106350.
428 Y. Li, M. Chen, B. Liu, Y. Zhang, X. Liang and X. Xia, *Adv. Energy Mater.*, 2020, **10**, 2000927.
429 C. Meng, X. Chen, Y. Gao, Q. Zhao, D. Kong, M. Lin, X. Chen, Y. Li and Y. Zhou, *Molecules*, 2020, **25**, 1136.
430 M. Crisci, F. Boll, S. Domenici, J. Gallego, B. Smarsly, M. Wang, F. Lamberti, A. Rubino and T. Gatti, *Adv. Mater. Interfaces*, 2025, **12**, 2400621.
431 J. Li, X. Yang, Z. Zhang, W. Yang, X. Duan and X. Duan, *Nat. Mater.*, 2024, **23**, 1326.
432 P. Ranadive, *Scalable Continuous Synthesis of Metal and Metal-Oxide Based Nanomaterials through Jet-Mixing*, The Ohio State University, 2021.
433 J. Kwon, S. Ko, H. Kim, H. J. Park, C. W. Lee and J. Yeo, *Mater. Chem. Front.*, 2024, 2322.
434 Y. Chen, F. Fang and N. Zhang, *npj 2D Mater. Appl.*, 2024, **8**, 17.
435 S. Lei, X. Zhao, X. Yu, A. Hu, S. Vukelic, M. B. Jun, H.-E. Joe, Y. L. Yao and Y. C. Shin, *J. Manuf. Sci. Eng.*, 2020, **142**, 031005.
436 E. H. Hill, *J. Mater. Chem. C*, 2024, **12**(30), 11285–11318.
437 K. Nasrin, V. Sudharshan, K. Subramani and M. Sathish, *Adv. Funct. Mater.*, 2022, **32**, 2110267.
438 L. Wu, Y. Li, Z. Fu and B.-L. Su, *Natl. Sci. Rev.*, 2020, **7**, 1667.
439 N. H. Solangi, A. Abbas, N. M. Mubarak, R. R. Karri, S. H. Aleithan, J. Kazmi, W. Ahmad and K. Khan, *Mater. Today Sustain.*, 2024, 100896.
440 J. Choi, K. Morey, A. Kumar, D. Neupane, S. R. Mishra, F. Perez and R. K. Gupta, *Mater. Today Chem.*, 2022, **24**, 100848.
441 H. Dai, L. Wang, Y. Zhao, J. Xue, R. Zhou, C. Yu, J. An, J. Zhou, Q. Chen, G. Sun and W. Huang, *Research*, 2021, **2021**, 5130420.
442 Y. Yang, B. Sun, Z. Sun, J. Xue, J. He, Z. Wang, K. Sun, Z. Sun, H. K. Liu and S. X. Dou, *Coord. Chem. Rev.*, 2024, **510**, 215836.
443 R. Maleki, M. Asadnia and A. Razmjou, *Adv. Intell. Syst.*, 2022, **4**, 2200073.
444 D. Y. Kirsanova, M. Soldatov, Z. Gadzhimagomedova, D. Pashkov, A. Chernov, M. Butakova and A. Soldatov, *J. Surf. Invest.: X-Ray, Synchrotron Neutron Tech.*, 2021, **15**, 485.
445 K. Choudhary, K. F. Garrity, S. T. Hartman, G. Pilania and F. Tavazza, *Phys. Rev. Mater.*, 2023, **7**, 014009.
446 M. A. F. Afzal and J. Hachmann, High-throughput computational studies in catalysis and materials research, and their impact on rational design, *World Sci.*, 2020, 1.
447 T. Zheng, Z. Huang, H. Ge, P. Hu, X. Fan and B. Jia, *Energy Storage Mater.*, 2024, 103614.
448 B. Sridharan, M. Goel and U. D. Priyakumar, *Chem. Commun.*, 2022, **58**, 5316.
449 Y. Yang, K. Yao, M. P. Repasky, K. Leswing, R. Abel, B. K. Shoichet and S. V. Jerome, *J. Chem. Theory Comput.*, 2021, **17**, 7106.

450 K. Shahzad, A. I. Mardare and A. W. Hassel, *Sci. Technol. Adv. Mater.:Methods*, 2024, **4**, 2292486.
451 F. Qayyum, D.-H. Kim, S.-J. Bong, S.-Y. Chi and Y.-H. Choi, *Materials*, 2022, **15**, 1428.
452 C. Xiouras, F. Cameli, G. L. Quilló, M. E. Kavousanakis, D. G. Vlachos and G. D. Stefanidis, *Chem. Rev.*, 2022, **122**, 13006.
453 A. Dhakal, C. McKay, J. J. Tanner and J. Cheng, *Briefings Bioinf.*, 2022, **23**, bbab476.
454 J. Li, K. Lim, H. Yang, Z. Ren, S. Raghavan, P.-Y. Chen, T. Buonassisi and X. Wang, *Matter*, 2020, **3**, 393.
455 X. Liu, K. Fan, X. Huang, J. Ge, Y. Liu and H. Kang, *Chem. Eng. J.*, 2024, 151625.
456 H. Xu, Z. Li, Z. Zhang, S. Liu, S. Shen and Y. Guo, *Nanomaterials*, 2023, **13**, 1352.
457 M. Karthikeyan, D. M. Mahapatra, A. S. A. Razak, A. A. Abahussain, B. Ethiraj and L. Singh, *Catal. Rev.*, 2024, **66**, 997.
458 S. Iravani, A. Khosravi, E. N. Zare, R. S. Varma, A. Zarrabi and P. Makvandi, *RSC Adv.*, 2024, **14**, 36835.
459 T. Ha, D. Lee, Y. Kwon, M. S. Park, S. Lee, J. Jang, B. Choi, H. Jeon, J. Kim and H. Choi, *Sci. Adv.*, 2023, **9**, eadj0461.
460 X. Zou, J. Pan, Z. Sun, B. Wang, Z. Jin, G. Xu and F. Yan, *Energy Environ. Sci.*, 2021, **14**, 3965.
461 H. Adamu, S. I. Abba, P. B. Anyin, Y. Sani and M. Qamar, *Energy Adv.*, 2023, **2**, 615.
462 W. Qiu, Y. Wang and J. Liu, *Wiley Interdiscip. Rev.: Comput. Mol. Sci.*, 2022, **12**, e1592.
463 G. Hyun, Y. Ham, J. Harding and S. Jeon, *Energy Storage Mater.*, 2024, **69**, 103395.
464 Y. Elbaz, D. Furman and M. Caspary Toroker, *Adv. Funct. Mater.*, 2020, **30**, 1900778.